Comparative Study of Green and Sol-Gel Synthesis of CaO NPs and Evaluation of Their Antibacterial Activities

Gezahegn Mengiste Bekele

A Thesis Submitted to the Department of Applied Physics

School of Applied Natural Science

Presented in Partial Fulfillment of the Requirement for the Degree of Master's in Applied Physics (Material Physics)

Office of Graduate Studies

Adama Science and Technology University

July, 2023

Adama, Ethiopia

Comparative Study of Green and Sol-Gel Synthesis of CaO NPs and Evaluation of Their Antibacterial Activities

Gezahegn Mengiste Bekele

Advisor:

Solomon Tiruneh Dibaba (PhD)

Co- Advisor:

Fekadu Tolessa (PhD)

A Thesis Submitted to the Department of Applied Physics

School of Applied Natural Science

Presented in Partial Fulfillment of the Requirement for the Degree of Master's in Applied Physics (Material Physics)

Office of Graduate Studies

Adama Science and Technology University

July, 2023

Adama, Ethiopia

Declaration

I hereby declare that this Master research thesis entitled "**Comparative study of Green and Sol-gel Synthesis of CaO NPs and Evaluation of their Antibacterial Activities**" is my original work which has not been submitted to any academic award degree or diploma for a similar purpose. All the references used in this research thesis are duly recognized by proper citations.

Student's Name: **Gezahegn Mengiste Bekele**

Signature: _____

This MSc thesis has been submitted for examination with our approval as thesis advisors.

Advisor's Name: **Solomon Tiruneh Dibaba (PhD)**

Signature: _____

Date of submission: _____

Recommendation of Advisors

I, the major advisor/supervisor of this research thesis, hereby certify that I have closely supervised the student while developing this thesis and read the draft thesis l entitled, "**Comparative study of Green and Sol-gel Synthesis of CaO NPs and Evaluation of their Antibacterial Activities**", prepared under my guidance by **Gezahegn Mengiste Bekele**. Therefore, I/we recommend the submission of the thesis to the department for further review and evaluation.

_____	_____	_____
Major Advisor	Signature	Date
_____	_____	_____
Co-advisor	Signature	Date

APPROVAL PAGE

I/we, the advisors of the thesis entitled "**Comparative study of Green and Sol-gel Synthesis of CaO NPs and Evaluation of their Antibacterial Activities**" and developed by **Gezahegn Mengiste Bekele** hereby certify that the recommendation and suggestions made by the board of examiners are appropriately incorporated into the final version of the thesis.

Major supervisor	Signature	Date
Co-advisor	Signature	Date

We, the assigned, members of the Board of Examiners of the thesis by **Gezahegn Mengiste Bekele** have read and evaluated his thesis entitled "**Comparative study of Green and Sol-gel Synthesis of CaO NPs and Evaluation of their Antibacterial Activities**" and examined the candidate during open defense. This is, therefore, to certify that thesis has been accepted in partial fulfillment of the requirements of the Degree of Masters of Science in Applied Physics (Material Physics).

Chairperson	Signature	Date
Internal Examiner	Signature	Date
External Examiner	Signature	Date

Final approval and acceptance of the thesis is contingent up on submission of its final copy to the office of Postgraduate Studies (OPGS) through the Department Graduate Council (DGC) and School Graduate Committee (SGC).

Department Head	Signature	Date
School Dean	Signature	Date
Postgraduate Dean	Signature	Date

ACKNOWLEDGEMENTS

First and foremost, thanks **Almighty God** for giving me strength and normal heath in the accomplishment of my thesis. And also I need to thank him made me kind to wonderful colleagues, experts, and friends nearby me up to the completion of my thesis work.

Next, I would like to express my heartfelt gratitude and deepest gratitude to my Advisor honorable **Dr. Solomon Tiruneh** for his inspiration, invaluable knowledge in the research area and sharing experience without any hesitation, Progressive encouragement; moral and technical support, constructive suggestions, and comments and his corrections on this research thesis have made this work fruitful. The care and his fatherly approach are very appreciable and are lucky to have him as my thesis advisor, indeed. In the same manner, I would like to extend my gratitude to my Co-advisor **Dr. Fekadu Tolessa** for his moral support, technical support on thesis, continuous encouragement, and invaluable comment in the successful completion of my thesis project.

Thirdly, I would like to express my special gratitude to my **Father and Mother** for their endless support starting from before and after the day when I come to this world. Their Praying to God, long wishes, and financial support all that they paid made me who I am today. And also thanks to my elder two sisters and three brothers for discharging responsibility as sisterly and brotherly manners which is expected from all of them. Above all, I have a special gratitude to my brother **Ketema Mengiste** who sacrifices more by giving inspiration and financial support for me to be successful in this thesis work. My final gratitude goes to Adama Science and Technology University (ASTU) for providing me the necessary financial support by office of Graduate studies (OFGS) **under Grant Number ASTU/SM-R/770/23** and laboratory facilities that are required to the accomplishment in the thesis work.

DEDICATION

This thesis work is dedicated to my beloved Mother **Elfinash Koru Jima.**

TABLES OF CONTENTS

LISTS OF FIGURES

FIGURES **PAGE**

LLISTS OF TABLES

TABLES PAGE

Acronyms and Abbreviations

MONPs..... Metal Oxide Nanoparticles

CaO.....Calcium Oxide

CuO.....Copper Oxide

ZnO.....Zinc Oxide

TiO_2.....Titanium Oxide

Al_2O_3.....Aluminum Oxide

MgO.....Magnesium Oxide

ZrO_2.....Zirconium oxide

CeO_2.....Cerium Oxide

$CaCO_3$.....Calcium Carbonate

$Ca(OH)_2$.....Calcium Hydroxide

$CaCl_2$.....Calcium Chloride

NaOH.....Sodium Hydroxide

HCl.....Hydrochloric Acid

XRD.....X-ray Diffraction

UV-Vis.....Ultraviolet-Visible Spectroscopy

PL.....Photoluminescence

SEM.....Scanning Electron Microscopy

TEM.....Transmission Electron Microscopy

TGA .....Thermogravimetric Analysis

DTA.....Differential Thermal Analysis

FWHW.....Full Width Half Maximum

MHA.....Muller Hilton Agar

Abstract

Synthesis of metal oxide nanoparticles by utilizing traditional medicinal plant extract is the promising alternative to the convectional chemical methods. This work aimed to synthesize calcium oxide nanoparticles through green approach using indigenous Moringa stenopetala leaf extracts as compared to sol-gel synthetic methods. The basic properties of green synthesized CaO NPs using Moringa stenopetala leaf extract and sol-gel method of CaO NPs has been studied by XRD, UV- Vis, PL, TGA, FTIR, and SEM. The XRD spectra showed that the synthesized CaO NPs via green approach were more crystalline and contained good purity as compared XRD patterns that obtained from the sol-gel synthesized CaO NPs. The average crystallite of CaO NPs obtained from XRD spectra using green synthesis method was found to be 13.59 nm. UV-Vis absorption spectra showed that the energy band gap of green synthesized and CaO NPs sol-gel which was found to 3.85 eV, and 3.78 eV respectively. The green synthesized CaO NPs lead to wide energy band gap as compared to sol-gel method synthesis due to the confirmation of small sized CaO NPs. Photoluminescence spectra analysis, the emission peak around 418.64 nm revealed that the green synthesized calcium oxide nanoparticles which are attributed to the radiative recombination of excitons. FT-IR analysis indicated that the presence of the functional group attached to the green synthesized of CaO NPs and sol-gel synthesis. The TGA analysis showed that the evaporation of water contents from the nanoparticles were at 400 ℃ and decomposition temperature of the dried $Ca(OH)_2$ gel occurred between 550 ℃ and 750 ℃, where the CaO NPs was synthesized. The total percentage weight loss of sample from 100 ^oC to 750 ^oC accounts for 16.471%. SEM analysis showed surface nature of green synthesized CaO NPs appeared as spherical shape and the average particles size found to be 24.15 nm. Similarly, the average size and shapes of particles observed using the sol-gel synthesized were recorded 90-110 nm and cubic phase nature respectively. The synthesized of CaO NPs via the green synthesis methods were applied on the gram positive bacteria (S. aureus, S. pyogenes) and gram negative bacteria (E. coli, P. aeruginosa) of 50mg/mL concentration, showed the inhibition zones (15.67±0.69 mm, 17.3±3.055 mm) and (20.75±1.56 mm, 19.6±2.460 mm) respectively.

Keywords: *Green synthesis, Moringa stenopetala, sol-gel, Calcium oxide nanoparticles, Antibacterial activity*

CHAPTER 1 - INTRODUCTION

1.1. Background of the study

Nanotechnology deals with the design, characterization, production, and application of structures, devices, and systems by controlling shape and size at the nanometer scale (Sorbiun et al., 2018). Nowadays, studying and deep understanding of the properties of nanomaterials bring about vast field applications of science and technology which widen new horizons for renewable energy, medical therapy, and human health. In nanomaterial universe, metal oxide nanoparticles received a lot of interest from scientists due to they exhibit distinct properties depending on their size, shape, stability, and uniformity formation (Kumar et al., 2021).

Owing to their large surface area to volume ratio and good reactivity in comparison to their respective bulk counterparts, metal oxide nanoparticles are considered to be more promising as they exhibit unique physical, chemical, and biological properties. Moreover; metal oxide nanoparticles synthesized through chemical methods are harmful and toxic to the environment due to the involvement of chemicals for reduction and capping agents as compared to green synthesis. Hence, the synthesis of metal oxide nanoparticles via plant extracts has received significant attention. In the green synthesis of metal oxides nanoparticles using plant extract, three important parameters are metal salt, a reducing agent, and a stabilizing or capping agent for modulating the size of nanoparticles and preventing their aggregation (Singh et al., 2018). Plant extracts contain various active biomolecules that help in the reduction and stability of nanoparticles (Demissie et al., 2020).

Amongst metal oxide nanoparticles, calcium oxide nanoparticles) is one of the predominant an alkaline earth metal oxide with a high dielectric constant of 11.8 and bulk wide band gap of 7.1 eV (Osuntokun et al., 2018). Due to unique chemical, physical, biological, and optical properties, CaO NPs have numerous applications like antibacterial agent, antifungal agent, potential drug delivery agent, tissue dissolution, photo thermal therapy, photodynamic therapy and synaptic delivery of chemotherapeutic agents (Eram et al., 2021). Calcium oxide nanoparticles synthesized via various methods including thermal decomposition methods (Alobaidi et al., 2022), sol-gel processing (Habte et al., 2019), Micro-assisted synthesis (Roy & Bhattacharya, 2011), direct precipitation (Kumar et al., 2021), ball milling (kimia et al, 2019), solvothermal (Marasini et al., 2020), physical methods (Chinthakuntla et al., 2015), green synthesis methods (Hadi & Mehdi, 2023; Mazher et al., 2023; Ramli et al., 2019), etc. Amongst all the aforementioned chemical routes, green synthesis plant extracts mediated is the more promising for the synthesis of CaO NPs due to an ecofriendly and easily available.

Recently, Calcium oxide nanoparticles have attracted much attention from researchers due to their application in wound dressings and bio-reduction properties, potential industrial use such as gas sensors, catalytic processes, high-temperature superconductors and solar cells (Gurav et al., 2020). With regards to the previous literature reports, CaO nanoparticles have been synthesized from various plant extracts like *Ocimum sanctum* (Gurav et al., 2020), *Moringa oleifera* (Jadhav et al., 2022), *Rhododendrum arboretum* (Ramola & Joshi, 2019), *Piper nigrum* (Mushtaq et al., 2022), *Carica papaya* and *Berberis vulgaris* (A.P. Sudha et al, 2020) and their antibacterial activities were also reported. Therefore, this study explored the use of *Moringa stenopetala* leaves extract in addition to its many other traditional applications as a capping and reducing agent for the synthesis of CaO-NPs. It also evaluated the antibacterial activities of the synthesized CaO NPs against pathogenic organisms using the agar disk diffusion method. In addition, this work opens the door for additional research on other indigenous Ethiopian plants for the synthesis of nanomaterials that might be employed for a variety of purposes.

In the present study, *Moringa stenopetala* leaf extracts were taken as a candidate for the synthesis of CaO nanoparticles. *Moringa stenopetala* is a class of the Moringaceae family and it is one of the species of the thirteenth Moringa genera. It is considered as the tradition medicinal endemic plant to Southern Ethiopia which can be used to antioxidant and antimicrobial properties. The leaf extract of *Moringa stenopetala* is rich in bioactive compounds such as flavonoids, phenols, and alkaloids, which can act as natural reducing and stabilizing agents during the synthesis of nanoparticles. Furthermore, *M. stenopetala* is used traditionally as food and to treat malaria, hypertension, asthma, diabetes, common cold, wounds, retained placenta and stomach problems (Hadis et al., 2020). Furthermore, the *M. stenopetala* possesses coagulant activity which is helpful for purifying water and antimicrobial potential (Duguma et al., 2022).

1. 2. Statement of the Problem

Most chemical and physical methods have been used for the synthesis of CaO nanoparticles such as thermal decomposition (Alobaidi et al., 2022), direct precipitation (Kumar et al., 2021), and sol-gel processes (Habte et al., 2019) and other else methods. Nevertheless, CaO nanoparticles have been synthesized via all these chemical routes, they are hazardous, consuming time reaction, and somewhat complicated process with compared to the green synthesis routes. To date, there are limited reports considering the green synthesis method. Apart from this, green synthesis of nanoparticles using aqueous plant extract is an environmentally friendly and cheap route to nanoparticle synthesis (Osuntokun et al., 2018). Particularly, CaO is intriguing due to being considered a benign chemical to human and animal species (Hadi et al., 2022). To the best of our knowledge, the use of *Moringa stenopetala* leaf extract for green synthesis of CaO nanoparticles with compared to the sol-gel synthesis CaO nanoparticles using calcium nitrate tetrahydrate as a source of calcium oxide has not been reported yet and it needs to be further investigation uniquely for antibacterial activities. More importantly, *M. stenopetala* aqueous leaf extract were suitable and capable of reducing agents and capping agents and rich secondary metabolites so that it produces calcium oxide from the precursor and exhibits the antibacterial activity.

1.3. Objectives of the Study

1.3.1. General Objective

The general objective of this study is the comparative study of green and sol-gel synthesis of Calcium Oxide nanoparticles for their antibacterial activities.

1.3.2. Specific Objectives

- To synthesize calcium oxide using the aqueous leaf extracts of *Moringa stenopetala.*
- To identify the crystallite size of CaO-NPs by using X-ray diffraction.
- To analyze morphology of CaO-NPs using scanning electron microscopy.
- To determine the absorption spectrum peak of CaO NPs using UV- visible spectroscopy technique analysis.
- To examine the antibacterial activity of calcium oxide nanoparticles using the agar disk diffusion method.

1.4. Significance of the Study

This study will be concerns about the green synthesis of calcium oxide nanoparticles using *Moringa stenopetala* aqueous leaf extract and the assessment of antibacterial activity under testing on various the bacterial cells. It will be expected to have significance such as increasing the public attention in the developments of green synthesis of calcium nanoparticles and the better understanding the synthesis of metal oxide nanoparticles. Furthermore, evaluation of CaO nanoparticles using the agar disk diffusion method allows it to permeate the bacterial cells and results in cell death. More importantly, the green synthesis of CaO nanoparticles is so eco-friendly, non-noxious, and less harmful to the environment and living organisms.

1.5. Scope of the Study

This research work will be delimited to comparative study of green and sol-gel synthesis of calcium oxide nanoparticles and evaluation of their antibacterial activities. These calcium nanoparticles can be characterized by using XRD, FTIR, SEM, PL, and UV-Vis Spectroscopy. Furthermore, the application of the bacterial activity was conducted via the agar disk diffusion method.

CHAPTER 2 - REVIEW OF RELATED LITERATURE

In this chapter, the theoretical concepts of nanoparticles, metal oxide nanoparticles, and synthesis approaches of metal oxide nanoparticles reviewed in the literature in detail. Besides, the fundamental properties of calcium oxide nanoparticles and their synthesis routes, characterization techniques, applications of calcium oxide nanoparticles and its antibacterial activity were briefly described.

2.1. Nanoparticles

Nanoparticles are particles that have at least one dimension in the nanometer range, typically between 1 and 100 nanometers (Nuryantini et al., 2019). Nanoparticles can be made from a variety of materials including metals, semiconductors, polymers, and ceramics. They can be engineered to exhibit unique physical, chemical, and biological properties that are different from their bulk counterparts. Because of their small size, nanoparticles have a high surface area-to-volume ratio, which can result in increased reactivity and different electronic, optical, and magnetic properties than their bulk counterparts. This makes them useful for a wide range of applications, including drug delivery, imaging, sensing, catalysis, and electronics. The small size of nanoparticles allows them to penetrate biological barriers and interact with cells and tissues in ways that larger particles cannot, which may have implications for their toxicity and safety.

2.1.1. Metal Oxide Nanoparticles

Metal oxide nanoparticles are made up of purely metallic elements (precursors) such as iron, calcium, magnesium, copper, zinc, titanium and etc.) combined with oxygen (Naseem & Durrani, 2021). The prominent semiconductor metal oxide (MO) nanoparticles including CuO, CaO, ZnO, SnO_2, Al_2O_3, MgO, ZrO_2, AgO, TiO_2 , CeO_2, Fe_2O_3 and TiO_2 (Ikram et al., 2022). They possess unique chemical, physical, and mechanical properties not seen in their bulk form, which makes them a subject of great interest in various scientific and industrial fields. Due to their small size and high surface area, these nanoparticles demonstrate superior catalytic activity, enhanced ability to absorb light, increased chemical reactivity, and improved electrical conductivity. They are used in a variety of applications, including electronics, energy storage, healthcare, environmental remediation, and nanotechnology-based consumer products.

2.1.2. Calcium Oxide Nanoparticles

Calcium oxide nanoparticles are nanometer-sized particles of metal oxide nanoparticles that exhibit unique properties as compared to their bulk counterparts. Calcium oxide also known as quicklime, is a caustic, alkaline, whitish chemical and the oldest known material that is used since the medieval age. It is a crystalline solid at room temperature having oxidation number +2 and belongs to the II-VI group of the periodic table. It is formed by an array of cations (Ca^{2+} ions) and anions (O^{2-} ions) having strong ionic bonding between them. However, the presence of moisture and water content in CaO converts it into slaked lime i.e. Ca $(OH)_2$. It exhibits semiconducting properties and remains chemically stable at very high temperatures. It is widely used in various fields as an efficient agent for ceramic, catalyst, cosmetic, waste remediation, destructive adsorbent for toxic chemicals and exhaust gases, targeted drug delivery, and refectory additive in paints (Gurav et al., 2020; Kumar et al., 2021).

Due to their small size and high surface-to-volume ratio, they have attracted attention in various fields, particularly in research that focuses on environmental remediation, biomedicine, agriculture, and antimicrobial activities. Among these applications, calcium oxide nanoparticles potential shifts to antimicrobial activities. The antimicrobial aspects of oxides have high microbial resistance and thermal stability as reported for various inorganic metal oxides MgO, ZnO and CaO NPs (Butt et al., 2015). Additionally, these nanoparticles can be used to deliver drugs to cancer cells, because they can penetrate the cell membrane and release their pay load in a targeted manner (Sarathy, 2018). Calcium oxide nanoparticles have also been investigated as contrast agents for medical imaging because they can absorb X-rays and enhance the visibility of tissues. In addition to catalysis and biomedicine, calcium oxide nanoparticles also have potential applications in environmental remediation and energy storage. Particularly, these nanoparticles can be used to remove pollutants from water and air and to store hydrogen in fuel cells.

2.3. Basic properties of Calcium oxide nanoparticles

2.3.1. Crystal structure of CaO NPs

The crystal structure of calcium oxide nanoparticles is a face-centered cubic (FCC) crystal structure. Each calcium ion is surrounded by six oxygen ions in an octahedral arrangement, and each oxygen ion is surrounded by four calcium ions in a tetrahedral arrangement. The crystal structure of calcium oxide nanoparticles was depending on aspects such as the unit cell, lattice parameters, and crystallite size.

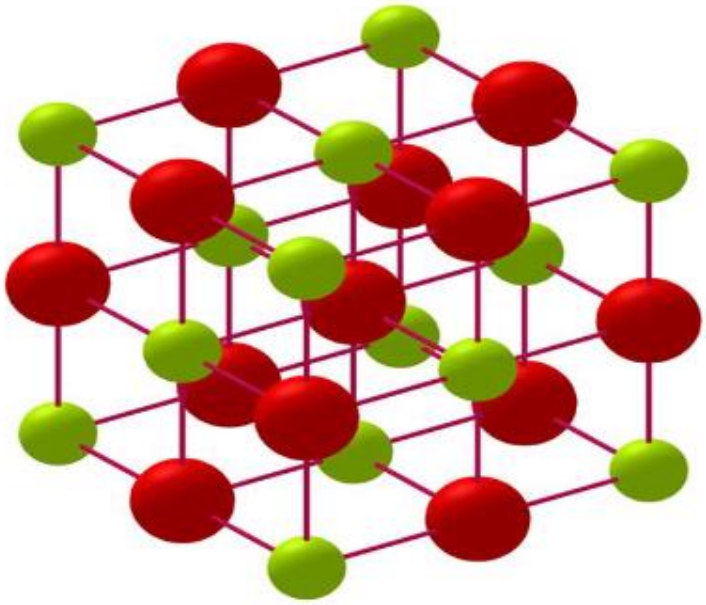

Figure 2.1: Crystal structure of Calcium Oxide nanoparticles with lattice constants, a = b = c = 4.8152 Å (Jadhav et al., 2022; Tang et al., 2013).

The lattice parameter (cell edge length) of the FCC unit cell for CaO nanoparticles is around 4.81 Å (angstroms). This value may slightly vary depending on the synthesis conditions and the presence of any impurities or defects within the crystal lattice. The lattice parameters determine the size and shape of the unit cell and have a significant impact on the properties of calcium oxide nanoparticles. The crystallite size of calcium oxide nanoparticles can range from a few nanometers to several hundred nanometers, depending on the synthesis conditions and processing methods.

The crystallite size can significantly affect the properties of CaO nanoparticles, such as the surface area, reactivity, and mechanical strength. Generally, smaller crystallites exhibit a

larger surface area and enhanced reactivity, making them more effective for applications such as catalysis, adsorption, and antimicrobial activities.

The surface structure of calcium oxide nanoparticles can be significantly different from the bulk crystal structure due to the presence of defects, impurities, unsaturated coordination sites, and surface reconstructions. These surface features play a critical role in determining the physicochemical properties and reactivity of CaO nanoparticles. For instance, the presence of defects and under-coordinated oxygen atoms on the surface can enhance the reactivity and catalytic activity of the nanoparticles.

The crystal structures can be analyzed by XRD which is governed by William Bragg's law expressed in Eqn (2.1) (Anowar Hossain, 2021).

According to Bragg's law

$$n\lambda = 2d\sin\theta \tag{2.1}$$

Where n is the order of diffraction (obviously, n=1), λ is the wavelength, 'θ' is the angle of diffraction, and'd' is the interspacing between the crystal arrangements having certain miller indices h, k, and l.

The average crystallite sizes of the synthesized nanoparticle can be obtained from the XRD peaks using by Debye- Scherrer equation Eqn (2.2) (M. Kumar & Ranjan, 2022).

$$D = \frac{K\lambda}{\beta_{hkl}\cos\theta} \tag{2.2}$$

Where, K is the shape factor, D is the average crystallite size of the particle, λ is the Cuk_{α} X-ray radiation wavelength, β is the light broadening width at half maximum in radians, and θ is the Bragg's angle of the diffracted planes.

Dislocation density, δ is a measure of the number of defects (specifically, dislocations) present in a crystalline structure. It is usually given in terms of dislocations per unit area (e.g., dislocations/m²). The dislocation density of nanoparticles varies significantly based on the synthesis method, the material composition, and size of the nanoparticle. It can be calculated using the crystallite size (D) using the relation equation in Eqn (2.3) (Zeid et al., 2019).

$$\delta = \frac{1}{D^2} \tag{2.3}$$

Microstrain (lattice strain) refers to the small changes or distortions in a crystalline material's lattice structure, which can result from various factors like mechanical stress, dislocations, impurities, or defects. It is used to discretize the lattice expansion of crystal structures. It is given by the Eqn (2.4) (Zeid et al., 2019).

$$\varepsilon = \frac{\beta \cos\theta}{4} \tag{2.4}$$

2.3.2. Electrical Properties

The electrical properties of calcium oxide nanoparticles can vary depending on their size, shape, and surface properties. Calcium oxide nanoparticles at the nanoscale and its electrical properties can change due to quantum confinement effects. The other study found that the conductivity of CaO nanoparticles was affected by the presence of surface defects and impurities. Several studies conducted the dielectric properties of CaO nanoparticles and found that their dielectric constant increased as the particle size decreased. The study attributed this effect to changes in the polarization and alignment of dipoles at the nanoscale. Calcium oxide nanoparticles have potential applications in various fields that require electrical properties. For example, these nanoparticles can be used as catalysts for electrochemical reactions, as well as in energy storage devices such as batteries and super capacitors. They can also be used in sensors and electronic devices, where their unique electrical properties at the nanoscale can enhance performance.

2.3.2.1. Energy Band gap of CaO NPs

The band gap of calcium oxide (CaO) nanoparticles can vary depending on their size and shape. The band gap is the energy difference between the top of the valence band and the bottom of the conduction band in a material. It is an important parameter that determines the electronic properties of a material, including its electrical conductivity and optical properties. The band gap of CaO nanoparticles decreased as the particle size decreased, due to the quantum confinement effect (Sumathi,et al, 2017). The study also found that the band gap of CaO nanoparticles was affected by the presence of surface defects and impurities. Also, the optical properties of CaO nanoparticles, and their absorbance and reflectance spectra varied with particle size. The study attributed these variations to changes in the band gap and the surface plasmon resonance of the nanoparticles. The band gap of CaO nanoparticles has potential applications in various fields, including electronics and energy conversion.

The band gap of CaO nanoparticles can be tuned by controlling their size and shape, which can be used to create materials with specific electronic and optical properties. These materials have potential applications in solar cells, where the band gap of the material can be optimized to match the solar spectrum for maximum efficiency.

There are two important types of band gaps in semiconductors, these are direct band gaps and indirect band gaps, as depicted in Figure 2.2. In direct band gaps, the minimum energy point in the conduction band has the same k value (crystal momentum) as the maximum energy point in the valence band, whereas in indirect band gap semiconductors which hasn't appeared in an indirect band gap semiconductor.

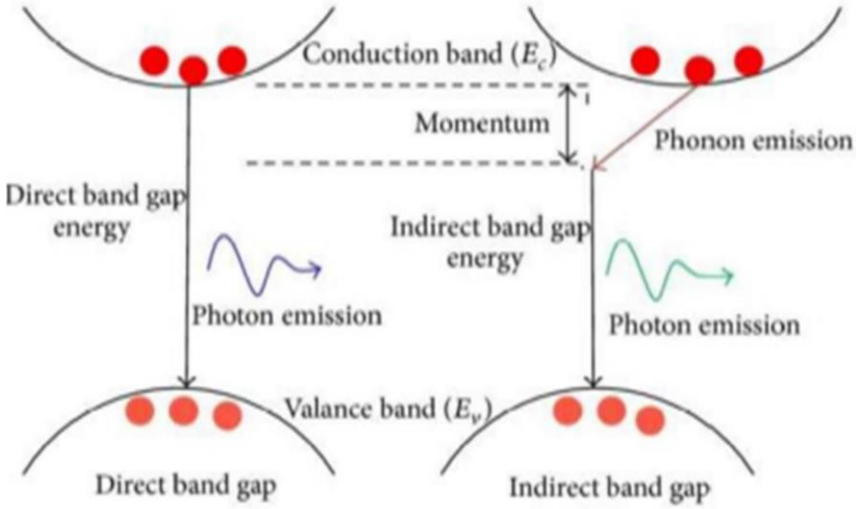

Figure 2.2: direct and indirect band gap of Semiconductor (Kebede Urge et al., 2023).

2.3.3. Optical properties of Calcium oxide nanoparticles

Calcium oxide nanoparticles possess unique optical properties that make them useful for various applications in science, technology, and medicine. The optical properties of CaO NPs can be characterized by their absorption, reflection, refraction, transmission, scattering, and luminescence properties. This property can be useful in various applications, such as UV-protection coatings or paints, antibacterial agents, and water purification systems. The absorption of light by CaO NPs can also result in photoluminescence or photo-thermal conversion, which can be harnessed for imaging and therapy in medical applications. The refractive index of CaO NPs increases with a decrease

in particle size, which can lead to higher reflection and scattering properties in the nanoscale. This property can be exploited to improve the opacity or hiding power of paints and thin films when CaO NPs are mixed with other materials, as well as enhance the reflectivity of surfaces for thermal management, lighting, or display applications. Due to their wide band gap, CaO NPs have high transparency in the visible and infrared regions of the spectrum. This property can be utilized in the fabrication of transparent and conductive electrodes, optical sensors, or catalysts that require light penetration or transmission.

The strong scattering properties of CaO NPs allow them to be effective in light-trapping or haze-inducing applications. These properties can be harnessed for energy-saving building materials, anti-reflective coatings, and window films to help reduce heat and glare while maintaining high optical transmittance. CaO NPs can exhibit photoluminescence which involves the absorption of photons and subsequent re-emission of light at lower energies. This property can be exploited for applications such as bio-imaging, photocatalysis, and security materials. By doping CaO NPs with rare-earth elements or other luminescent agents, their emission spectra can be tuned for a specific wavelength. CaO NPs have shown potential in nonlinear optics due to their large band gap, high optical transparency, and refractive index tunability. Applications of nonlinear optical properties include optical switches, modulators, and wave guides for integrated photonic devices and telecommunication systems.

2.4. Critical Approaches for synthesizing nanoparticles

2.4.1. Top-down approach

The top-down approach involves the reduction of a larger material into smaller nanoparticles through physical or chemical means. This can be achieved by techniques such as milling, lithography, or chemical etching. The starting material is typically a bulk material, and the process involves breaking it down into smaller particles until the desired size is achieved.

2.4.2. Bottom-up Approach

The bottom-up approach involves the assembly of smaller building blocks into larger nanoparticles through chemical reactions. This typically involves starting with molecular or atomic components and building up the structure through chemical synthesis. All methods commenced with the liquid and the gas belongs to this approach namely physical

vapor deposition (PVD), chemical vapor deposition (CVD), Sol-gel processes, wet chemical method, self-assembly, and green synthesis method. It also maintains good control for the morphology of nanoparticles.

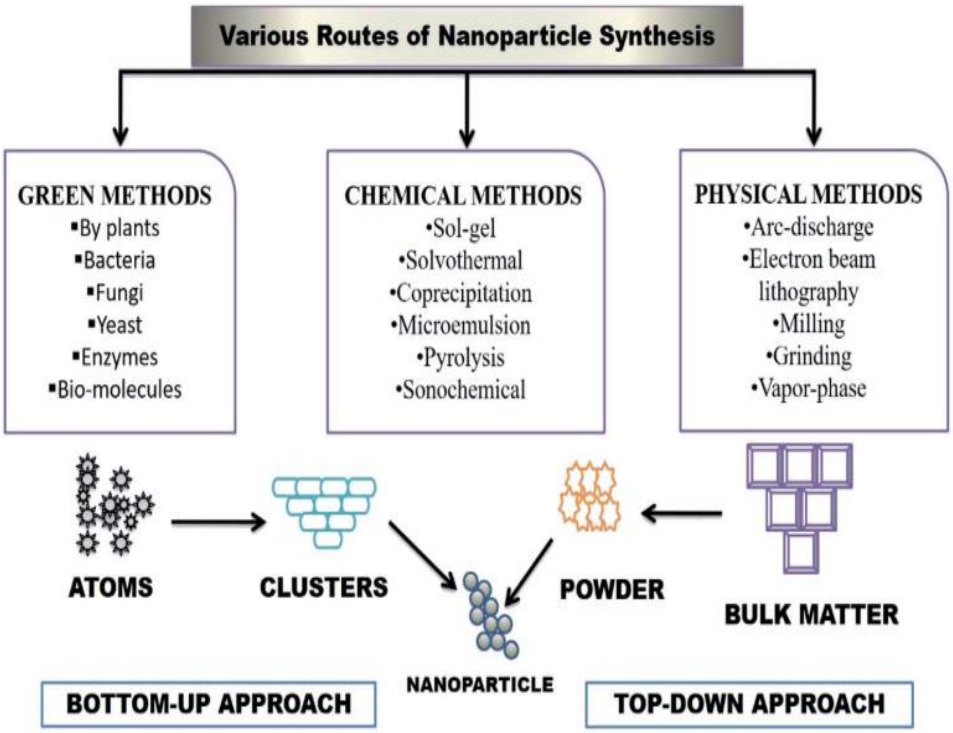

Figure 2.3: Novel Synthesis Methods of Nanoparticles (K. R. Singh et al., 2021).

2.5. Novel methods used to Synthesize Calcium Oxide Nanoparticles

2.5.1. Sol-gel process

Sol-gel method is a chemical process for making ceramics, glasses, and composite materials from precursor solutions (sol) that undergo a sol-to-gel transformation and ultimately to a solid material (gel). The sol-gel process involves the formation of a colloidal suspension (sol) of nanoparticles in a liquid, followed by gelation to form a three-dimensional network of particles, and finally drying and calcination to obtain a solid material. Sol-gel processes are so cheap and alternative way of synthesizing calcium oxide nanoparticles with controlled composition and morphology. Calcium oxide nanoparticles were produced from the waste egg shells through sol-gel methods (Habte et al., 2019). In this process, CaO nanoparticles were synthesized by sol-gel method in which raw eggshell

was dissolved by HCl to form $CaCl_2$ solution, adding NaOH to the solution dropwise to agitate $Ca(OH)_2$ the gel and finally drying the gel at high temperature.

2.5.2. Thermal Decomposition Method

The thermal decomposition method is a physical method used for the synthesis of calcium oxide nanoparticles. This method undergoes three processes preparation of precursor, heating, and cooling of the obtained calcium oxide nanoparticles after calcination. Physical methods include thermal decomposition sonochemical methods and microwave processing (Alobaidi et al., 2022). Among those methods, thermal decomposition was the preferred route to other methods in terms of synthesizing of calcium oxide nanoparticles from the chicken eggshells.

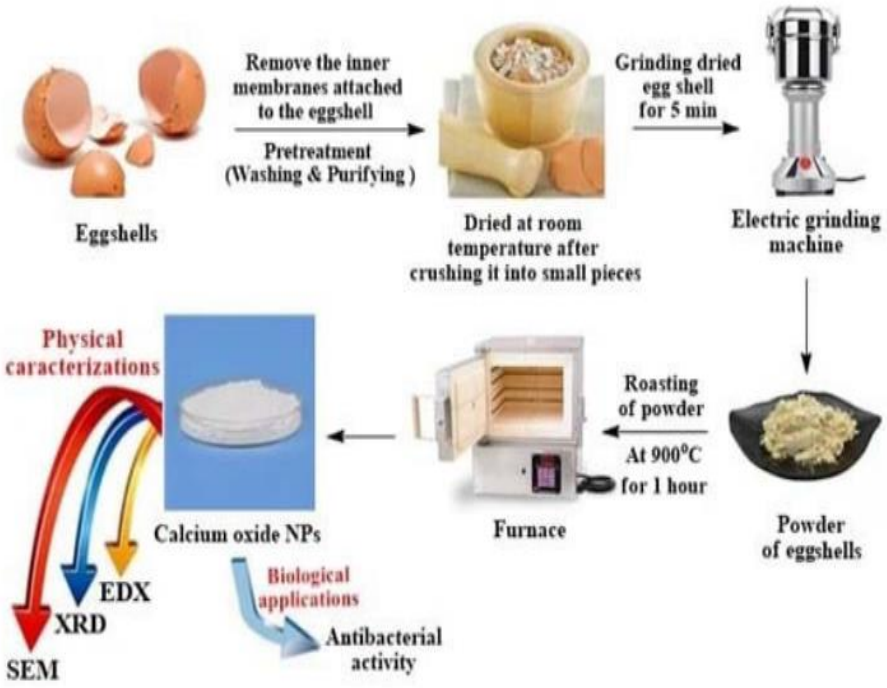

Figure 2.4: Thermal decomposition synthesis and application of CaO-NPs (Alobaidi et al., 2022).

2.5.3. Green synthesis of calcium oxide nanoparticles using Plant extracts

Green synthesis of calcium oxide nanoparticles (CaO NPs) refers to a sustainable and eco-friendly approach to fabricating nanoparticles using biological resources such as plant extracts. In the case of plant leaf extract, the process involves using calcium nitrate tetrahydrate as a precursor to creating CaO NPs. The green synthesis process starts by preparing a solution of calcium nitrate which acts as the source of calcium ions (Ca^{2+}). Subsequently, plant leaf extract is added to the solution under continuous stirring. The

mixture is then subjected to heat treatment, which triggers the biochemical reactions between the calcium ions and the phytochemicals present in the leaf extract. This process results in the reduction of calcium ions and their subsequent conversion into calcium oxide nanoparticles. The CaO NPs formed are stabilized by the bioactive compounds present in plant leaf extract, which prevent the nanoparticles from aggregating over growing in size. The synthesized nanoparticles are then isolated and purified by means of centrifugation and washing. The use of plant leaf extract not only provides an eco-friendly method for the synthesis of CaO NPs, but also lends additional benefits such as enhanced biological properties of the nanoparticles for potential biomedical application.

2.6. Characterization Techniques of Calcium oxide Nanoparticles

To employ calcium oxide nanoparticles for any area of applications, characterization techniques should be required instantly after the synthesis of the material. Different tangible techniques have been established to characterize the size, morphology, composition, and novel properties of calcium oxide nanoparticles. The most commonly employed for characterization techniques include the X-ray Diffraction, Photoluminescence Spectroscopy, UV-Visible Spectroscopy, Fourier Transform Infrared Spectroscopy, Thermogravimetric Analysis, Scanning Electron Microscopy and the others.

2.6.1. Photoluminescence Spectroscopy

Photoluminescence is a spectroscopic technique that involves the excitation of nanoparticles by a high-energy light source, typically a laser, followed by the emission of light at lower energy levels. The emitted light is typically in the visible or near-infrared range, and its intensity and spectral shape depend on the size, shape, and surface properties of the nanoparticles. PL spectroscopy can provide information about the energy levels and band gap of nanoparticles, as well as the presence of defect states and impurities. It is particularly useful for the characterization of semiconductor nanoparticles, such as quantum dots, which exhibit size-dependent optical properties.

2.6.2. Ultraviolet-Visible Spectrometry

UV-Vis spectrometry measures the absorption of light by a sample over a range of wavelengths from ultraviolet to visible. It can provide information about the electronic transitions and band gap of nanoparticles, as well as their size and shape. UV-Vis spectroscopy is often used to determine the concentration of nanoparticles in solution, as

well as to monitor their stability and aggregation behavior. It is also used to characterize the optical properties of nanoparticles such as their plasmonic resonance, which is important for applications such as sensing and photocatalysis.

The absorption peaks in UV spectroscopy depend on several factors such as chosen wavelength, electronic structure, band gap, oxygen vacancies, size, sample concentration, impurity, surface nature, and temperature. The optical energy band gap of a material is the minimum amount of energy needed to excite an electron from its ground state (E_1) in the valence band to a higher-energy state (E_2) in the conduction band. This transition allows the absorption of a photon, which gives rise to the material's optical properties. The band gap energy can be determined by replacing the value of the specific wavelength of relatively high absorption peaks in the following Eqn (2.5) (Kebede Urge et al., 2023).

$$E_g = E_2 - E_1 = h\vartheta = h\frac{c}{\lambda} = \frac{1240\ (nm.eV)}{\lambda_{max}\ (nm)} \qquad (2.5)$$

Where E_g is the band gap energy (eV), h is Planck's constant (4.135667×10^{-15}eVs), c is the speed of light ($3\times 10^{8} m/s$), λ is the absorption wavelength.

The optical band gap of E_g is determined by using a Tauc's plot (Osuntokun et al., 2018) as the following relation, Eqn (2.6) (Jubu & Muhammad, 2023).

$$(\alpha h\vartheta)^{\gamma} = A(h\vartheta - E_g) \qquad (2.6)$$

Where, γ is the nature of electron transition, α is the absorption coefficient, h is the plank's constant, ϑ is the photon's frequency, A is the proportionality constant, and E_g is the band gap energy.

2.6.3. X-ray Diffraction

X-ray diffraction is a non-destructive analytical technique that provides detailed information about the crystallographic structure, chemical composition, and physical properties of materials, including nanoparticles. In the context of nanoparticles, XRD characterization is essential to understand their phase, size, shape, and distribution, among other crucial properties affecting their performance and application. The broadening of the

XRD peaks can be used to estimate the size of the crystallites in the nanoparticle samples. This is typically done using the Scherrer formula, which relates the full-width at half-maximum of the diffraction peaks to the average size of the crystallites. By analyzing the broadening of multiple peaks, the size distribution of the nanoparticles can also be inferred, providing a deeper understanding of their properties and potential applications. The positions of diffraction peaks also reveal information about the lattice parameters of the unit cell forming the nanoparticles. By comparing the experimental and standard values of lattice parameters, one can deduce the presence of internal stresses or strains in the sample. This can arise from effects such as particle size reduction, the presence of defects, or the incorporation of impurities in the lattice.

2.6. 4. Fourier Transform Infrared Spectroscopy

FTIR analysis provides information about the chemical composition and functional groups of the surface of the nanoparticles. In FTIR analysis, a beam of infrared radiation is passed through the sample, and the amount of radiation absorbed by the sample is measured as a function of frequency. The resulting spectrum provides information about the vibrational modes of the chemical bonds within the sample, which are characteristic of the functional groups present. In the case of calcium oxide nanoparticles, the FTIR spectrum typically shows the presence of hydroxyl (OH) groups, which are commonly formed on the surface of the nanoparticles due to their interaction with water and moisture in the air. The FTIR spectrum of calcium oxide nanoparticles typically shows a broad band in the region of 3400-3600 cm^{-1} which is attributed to the stretching vibration of the hydroxyl groups. In addition, the FTIR spectrum may also show other bands corresponding to carbonates (CO_3^{2-}) or other impurities that may be present on the surface of the nanoparticles (Atchudan et al., 2022).

2.6.5. Scanning Electron Microscopy

Scanning electron microscopy is a powerful imaging technique that can be used to characterize the size, morphology, and surface features of calcium oxide nanoparticles. SEM analysis involves scanning a focused beam of electrons over the surface of the sample and detecting the secondary electrons that are emitted from the surface. The SEM image of CaO nanoparticles typically shows a range of particle sizes and shapes, depending on the method of synthesis and processing. The nanoparticles may appear as individual particles or as aggregates or clusters of particles. The image can provide

information about the size distribution of the nanoparticles, as well as their morphology and surface features, such as cracks, voids, or surface coatings.

2.6.6. Transmission Electron Microscopy

When the electron beam is transmitted through the sample, it interacts with the atoms in the calcium oxide nanoparticles and is scattered in different directions. The scattered electrons pass through a series of electromagnetic lenses, which focus the electrons onto a fluorescent screen or a digital detector to form an image of the sample. By analyzing the TEM images, it can be possible to determine the size, shape, and crystal structure of the calcium oxide nanoparticles. The crystal structure of the nanoparticles can be determined from the electron diffraction pattern, which is generated when the electrons interact with the crystal lattice of the nanoparticles.

2.7. Applications of metal oxide nanoparticles

Nanoparticles smaller than 100 nm interact with bacteria and produce electronic effects which improve the reactivity of nanoparticles. Thus, it is proven that the bactericidal effect of nanoparticles is size dependent. The cell membranes of the microorganisms interact with the medium, so metal NPs will have some interactions to release metal ions that interfere with the processes of the DNA replication, cell membrane formation, cell division, and so forth, of certain microorganisms such as bacteria, which results in an antimicrobial effect (Sorbiun et al., 2018). The antimicrobial activity of nanoparticles has largely been studied with human pathogenic bacteria such as *Escherichia coli* and *Staphylococcus aureus*. Because of these microbes seem to be highly sensitive to ZnO MgO, CuO, and CaO nanoparticles. The bactericidal activity of such nanoparticles in part depends on size, stability, and concentration in the growth medium (Azam et al., 2012).

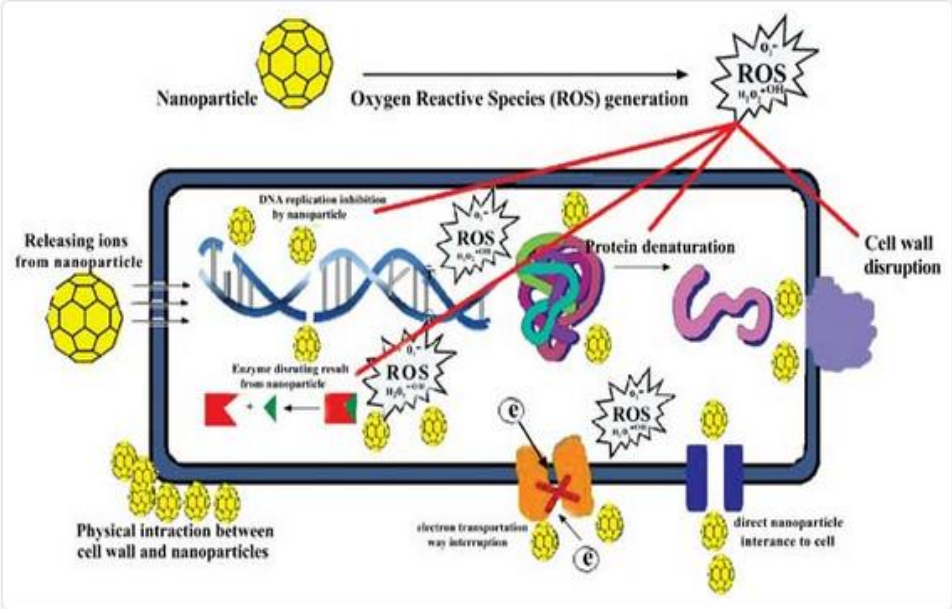

Figure 2.5: Plausible mechanisms of antibacterial activity of metal nanoparticles (Hoseinzadeh et al., 2017).

2.7.1. Antibacterial activities of CaO NPs

Calcium oxide nanoparticles have been shown to exhibit antibacterial activity against a wide range of bacteria. The antibacterial activity of CaO nanoparticles is attributed to their alkaline nature, which can disrupt bacterial cell membranes and cause cell death. In addition, the small size of the nanoparticles allows them to penetrate bacterial cells more easily than bulk CaO NPs. CaO nanoparticles were effective against both Gram-positive and Gram-negative bacteria, including Staphylococcus aureus and Escherichia coli (Kumar et al., 2021). The study found that the antibacterial activity of CaO nanoparticles increased with decreasing particle size, due to the increased surface area-to-volume ratio.

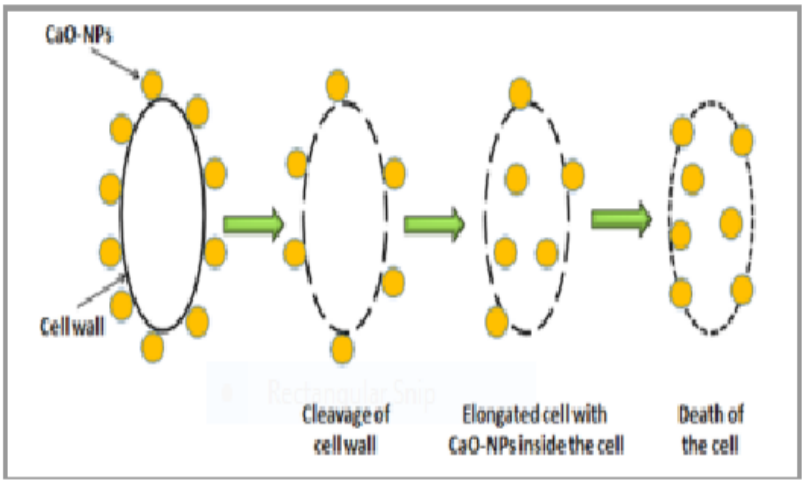

Figure 2.6: Interaction mechanisms of CaO NPs with bacterial cell membrane structure (Roy et al, 2013).

2.8. Disk diffusion method

The Disc-diffusion is perhaps the most used method for determining antibiotic resistance in the microbiological community because it is more practical, effective, simple, and inexpensive as compared to the agar disk diffusion method. This suspension is then uniformly dispersed onto a suitable agar (Müller-Hinton agar) in a Petri dish with a pH range of 7.2–7.4. Then, disks will be saturated with various well-defined quantities of various nano antimicrobials added to the agar surface. The placing of the discs could be accelerated by a multichannel disc dispenser. Zones of growth inhibition around each of the discs are measured after 16-24 hrs of incubation at 37°C (Shakhatreh et al., 2016). Susceptibility to that antibacterial will be shown by a distinct circular zone of no progress close to a disc. The size of the NPs, the pace of diffusion, the porosity of the agar, and potential charge interactions between the antimicrobial and the agar could all have an impact on the diffusion and ultimate size of the inhibitory zone. The highest concentrations should be close to the antimicrobial-containing disc and should be diffused away from the center.

CHAPTER 3 - MATERIALS AND METHODS

3.1. Materials and Chemicals

The materials (apparatus) used for the green synthesis included: Fresh leaves of *Moringa stenopetala*, a beaker, a magnetic stirrer, a hot plate, an incubator, power supply, a thermometer, Whatman No. 1 filter papers, digital electronic analytical balance (Model FA2104, China), furnace (Model BK-5-12GJ), ceramic crucible cups, drying oven (Model 101-0, Biobase Biodustry, Shandong Co. Ltd, China), cylinders, and centrifuge (Model AVI-558, max RPM: 5,000 rpm).

The chemicals and solvents required for the synthesis were listed as follows: Calcium nitrate tetrahydrate $Ca(NO_3)_2.4H_2O, 99.05\%$ Purity) (molar: 235.15g/mol), Merk Life Science, PLC), deionized water, ethanol, sodium hydroxide (NaOH), dimethyl sulfoxide (DMSO, $(CH3)_2OS$, 99.9% pure, Loba Chemie Pvt. Ltd., India). Calcium nitrate tetrahydrate was provided as precursors and sodium hydroxide was used for controlling the pH values. All the reagents used in the experiments would be in analytical grade and used without any further purification.

3.2. Instruments

The laboratory instruments employed for characterizing the CaO Nanoparticles were: X-ray Diffraction (XRD), (XRD-700x-Ray Diffractometer Maxima, Shimadzu Corporation, Japan), UV-Visible (UV-Vis) spectroscopy (Double Beam Spectrophotometer S-1600 Spectrophotometer India), Fourier Transform Infrared Spectroscopy (FTIR) (Perkin Elmer, Spectrum 65 FT-IR), and Photoluminescence (PL) (Model, MY18490002, Cary Eclipse, Fluorescence Spectrophotometer, Agilent Technologies, Malaysia).

3.3. Methods

3.3.1. Preparation of M. stenopetala leaves extraction

To begin with, the fresh leaves of *M. stenopetala* were collected from local farms (Konso, Southern Ethiopia*).* Then, the *M. stenopetala* sample was cleaned thoroughly with tap water and extremely wet in distilled water for 15 min and then rinsed with ethanol several times in order to eliminate dust materials present on the outer layer of leaves (sample). The leaves were completely air-dried for several days until the moisture contents were entirely evaporated. The dried leaves were grounded into coarse powder using a mortar and pestle. Later, 12 g of the powder of the sample was heated in beaker at 50 ^{o}C for 30 min in 120 mL of deionized water (DW). Lastly, after it has been cooled, the extracts solution is filtered with the Whatman No. 1 filter paper and kept in a refrigerator (2 °C to 4 °C) for further analysis. All these steps clearly displayed in Figure (3.1) below.

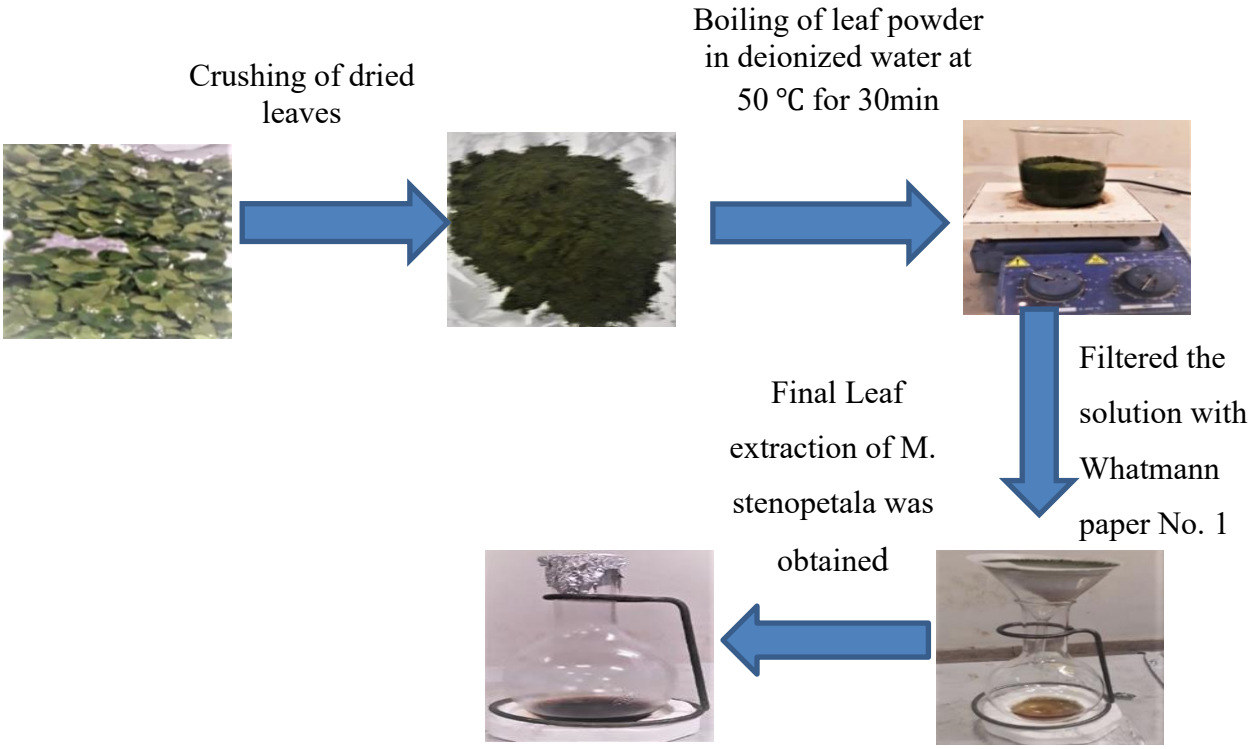

Figure 3.1: Preparation of Moringa stenopetala leaves Extraction

3.3. 2. Synthesis of Calcium oxide Nanoparticles

3.3.2.1. Green synthesis method

To perform the synthesis of calcium oxide nanoparticles, six grams of Calcium nitrate tetrahydrate ($6g\ of\ Ca(NO_3)_2.4H_2O$) was added to 100 mL of deionized water (DW). Then after, the uniform solution of calcium nitrate tetrahydrate was obtained by using the maginetic stirrer on the hot plate at room temperature. Of the 100 mL prepared solution, 50mL of $Ca(NO_3)_2.4H_2O$ was used. Later, 10 mL of leaf extracts were gradually added to 50ml calcium nitrate tetrahydrate solution in a beaker placed on hot plate by increasing temperature**.** Sodium hydroxide **(**2M, NaOH) was added dropwise to the solution to optimize the precipitation of $Ca(OH)_2$ and adjust the pH of the solution to 12. The mixtures were heated and stirred on a magnetic stirrer for 2 hr at 60°C. The yellow paste precipitate appeared with the addition of sodium hydroxide. Afterward, the solution left undisturbed (aging) overnight. Then, the pellets were centrifuged three times for 15 min intervals at 5,000 rpm and dried in an oven 100^{o}C for 10hrs. Finally, the dried sample was calcined in a muffle furnace at 500°C for 3 hr and the powder was collected for characterization. Figure 3.2 represents the schematics of synthesized CaO NPs using *M. stenopetala* leaves extracts.

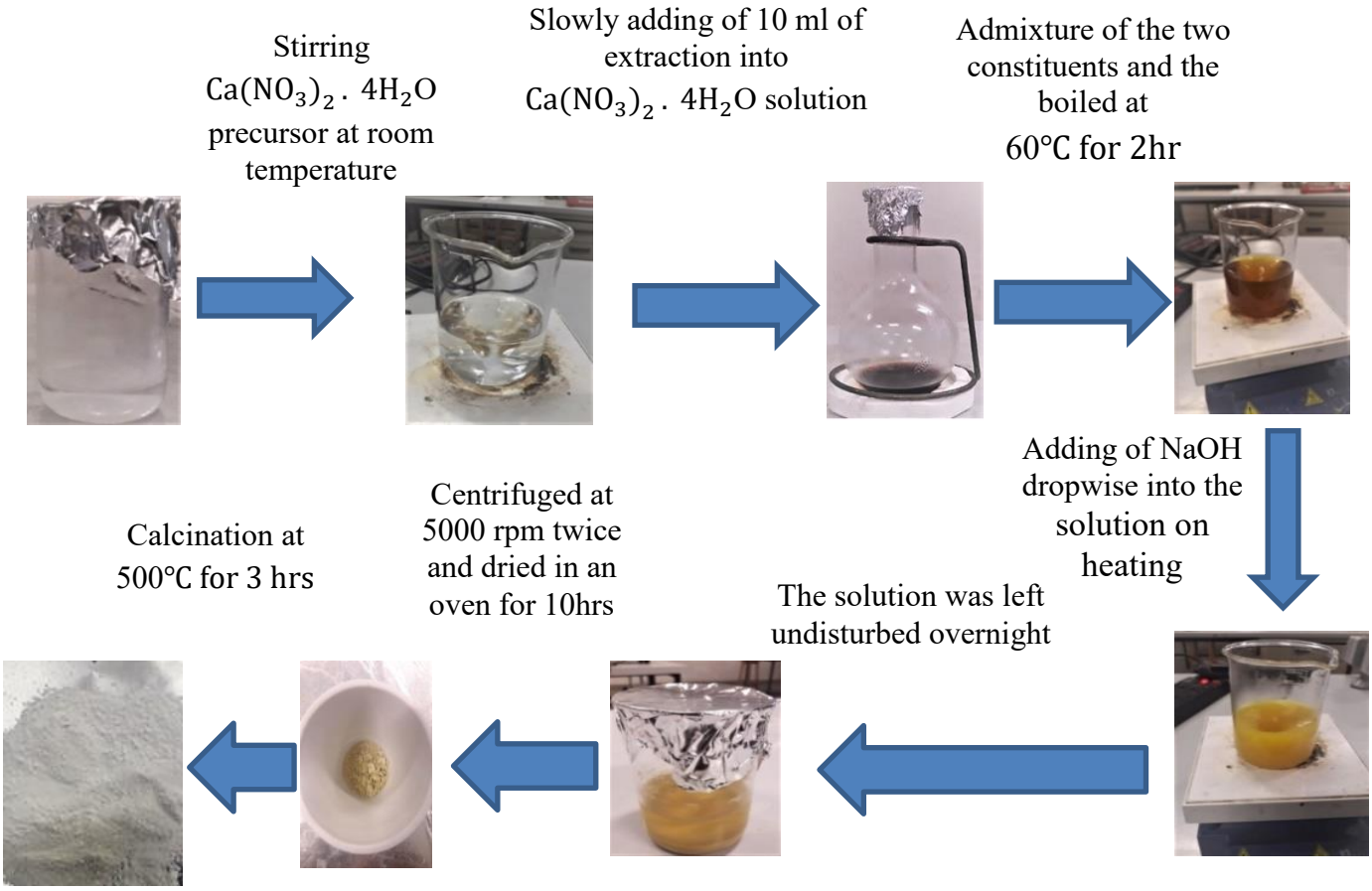

Figure 3.2: Green synthesis method of CaO NPs using *M. stenopetala* leaf extracts

3.3.2.2. Sol- gel method

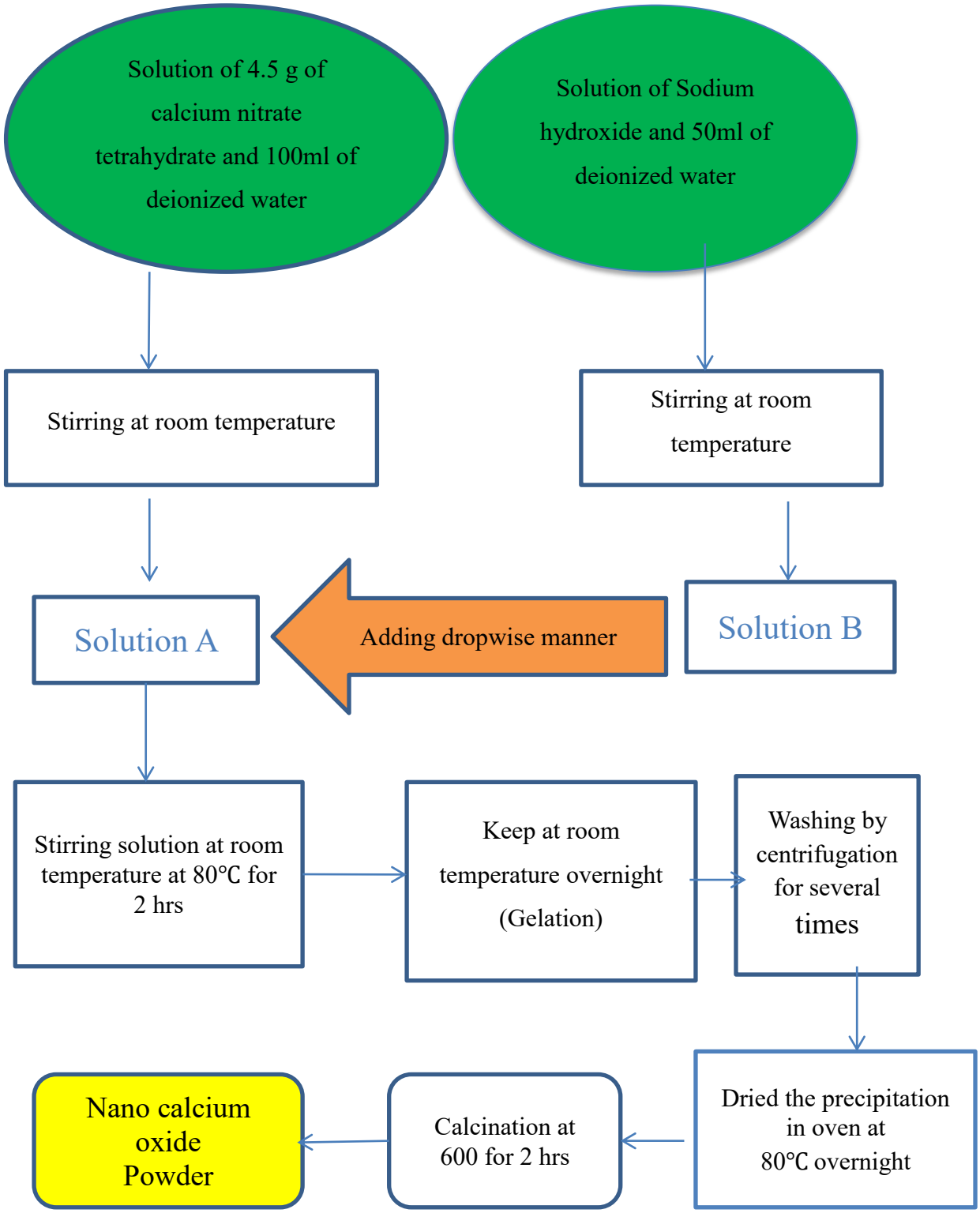

Figure 3.3: Schematic diagram of Sol-gel method synthesis of Calcium Oxide NPs

3.4. Methods of characterization

The x-ray diffraction pattern of Calcium oxide nanoparticles was recorded on (X-RAY DIFFRACTOMETER MAXIma) which is equipped with Cuk_{α} radiation ($\lambda = 0.154056$ nm) and operates at a voltage of 40 kV and applied current of 30mA in the scanning speed of 3 degrees per minute which makes the gathered data were scanned at a range of $2\theta = 10^{o} \leq 2\theta \leq 80^{o}$. The ASCII of files measured spectra were collected by the computer interfaced with the instrument and it was analyzed only through **Origin 2018 Software**. This technique helps to determine the plane spacing crystallite size, lattice parameters, dislocation density, and microstrain of green and sol-gel synthesized calcium oxide nanoparticles by using the equations expressed in Eqns (2.1-2.6).

The UV-Vis absorption peaks were inscribed with UV-Vis spectroscopy in the wavelength range of 200- 800 nm at room temperature. The calcium oxide nanoparticles synthesized via *Moringa stenopetala* leaf extract and sol-gel method were taken and dissolved in DMSO and transferred to 1cm quartz cuvette, then their absorbance would be measured. The numeric data of wavelength corresponds to the absorbance collected by the computer interconnected to the instrument. These recorded data are being analyzed by the origin 2018 software. The absorption peaks and optical energy band gap of calcium oxide nanoparticles can be calculated in accordance with equation expressed in Eqn (2.5).

The emission spectra of Calcium oxide nanoparticles were measured with Fluorescence Spectroscopy (Cary Eclipse, Fluorescence Spectrophotometer) at room temperature. Before conducting the measurements, the CaO NPs samples were rigorously shaken and uniformly dissolved in dimethyl sulphoxide after they had been measured by Digital electrical analytical balance. Like UV- Vis spectrophotometry, the spectra of samples were measured by using a 1cm quartz cuvette. The excitation wavelength of the samples was calibrated at 325 and 320 nm respectively for green synthesized and sol-gel method synthesized calcium oxide nanoparticles and the emission wavelength range of 400 – 450nm was observed with the slit width of an instrument adjusted to 10nm.

Calcium Oxide nanoparticles which produced via green synthesis and sol-gel methods were also characterized by Thermo gravimetric Analysis. Decomposition temperatures of $Ca(OH)_2$ gel were analyzed by thermogravimetric analysis (Shimadzu DTG-60H) in a platinum crucible at heating rate of 10 ℃/min from ambient temperature to 24℃ −800℃.

Initially, calcium oxide samples were prepared and it was dispersed in suitable solvents to assure the uniform distribution of nanoparticles and the solvent parts were dried and removed. Subsequently, the TGA instrument would be calibrated compared with the standard samples. The mass of calcium oxide was measured by milligram and loaded on a sample holder (crucible or pan) and located in the instrument. The equal masses of calcium nanoparticles were weighted and found to be 8.506 mg. The temperature ranges of the samples are 0 ℃ to 800 ℃ at a flowing rate of 50 ml per min. The mass change of the samples was performed as function of temperature and time.

3.5. Assessing of antibacterial test of Green synthesized and Sol-gel synthesized Calcium Oxide Nanoparticles

The antibacterial activity of green synthesized and sol-gel synthesized calcium oxide nanoparticles (CaO NPs) with various bacterial strains of gram-positive bacteria (Staphylococcus aureus (S. aureus)) (ATCC 25923), (Staphylococcus pyogenes (S. pyogenes)) (ATCC 19615) and gram-negative bacteria (Escherichia coli (E. coli)) (ATCC 25922), (Pseudomonas aeruginosa (P. aeruginosa)) (ATCC 27853) was determined using agar disk diffusion method. The microbial strains were grown in nutrient broth aerobically at 37℃ for 18-24 hrs until the turbidity of bacteria suspension achieved 1.5×10^{8} CFU/mL which is equivalent to 0.5 McFarland standards. 0.01 sub-cultured bacteria test pathogens were seeded using sterilized cotton swabs on sterilized molten and cooled MHA media and TSA respectively. Thereafter, a 6mm diameter sterilized Whatman filter paper discs were impregnated with different concentrations of green synthesized and sol- gel method of CaO NPs 50 mg/mL, 25mg/mL, 12.5mg/mL, and 6.25 mg/mL of each of the solvent fractions and standard antibiotic disc (1mg/ml of ciprofloxacin)., Using sterile forceps, each impregnated discs were transferred into each Petri dishes seeded (inoculated plate) with the bacterial strains. Then, it was left undisturbed for 30 min at room temperature so that it diffused on the plate. After half minute the plates containing the strains with nanoparticles were incubated at 37 ℃ for 24 hrs and placed upside down (inverted position). After incubation, the plates were evaluated for clear zone formed around the disks. Finally, each zones of inhibition of nanoparticles was measured using a ruler in (mm) and the mean values of each organism were noted. In the end, they compared it with standard antibiotic (ciprofloxacin).

CHAPTER 4 -RESULTS AND DISCUSSION

In this chapter, the results and discussions of the carried out experiments has been discussed. The first section of this chapter introduced the basic crystal structure as well as the lattice microstrain and the dislocation density of the green synthesized and sol- gel synthesized CaO NPs. In the second section of this chapter, the absorption spectra of the synthesized CaO NPs were clearly described. In the second section of this chapter, the photoluminescence spectra of with a different excitation wavelength of green synthesized and sol-gel synthesized CaO NPs were also elaborated. In the fourth section, the thermal analysis and also the morphology of CaO NPs were analyzed by TGA and SEM respectively. In the end and fifth section, the antibacterial activity of green synthesized and sol-gel synthesized CaO NPs clearly stated.

4.1. X-ray Diffraction (XRD) analysis

X-ray diffraction measurements have been used to analyze the crystalline size and the distinct properties of calcium oxide nanoparticles synthesized using *Moringa stenopetala* leaves extracts as compared with sol gel synthesized of calcium oxide nanoparticles utilizing calcium nitrate tetrahydrate as a precursor. Based on these routes, the observed diffraction peaks from green synthesized calcium oxide nanoparticles were 23.069º, 29.402º,32.1°, 36.0378º, 39.476º, 43.256, 47.427, 48.538º, 57.520º, and 64.960º indexed to (012), (011), (111), (113), (202),(116), (018) , (122) and (311). The most prominent peaks appeared at 2θ = 29.402º, 39.476º and 48.538º which are attributed to (011), (113) and (018) which agree with the same finding of CaO NPs (Ikram et al., 2022). Furthermore, the most intense XRD spectra clearly show that the highly crystalline and purity of the calcium oxide (CaO) nanoparticles**.**

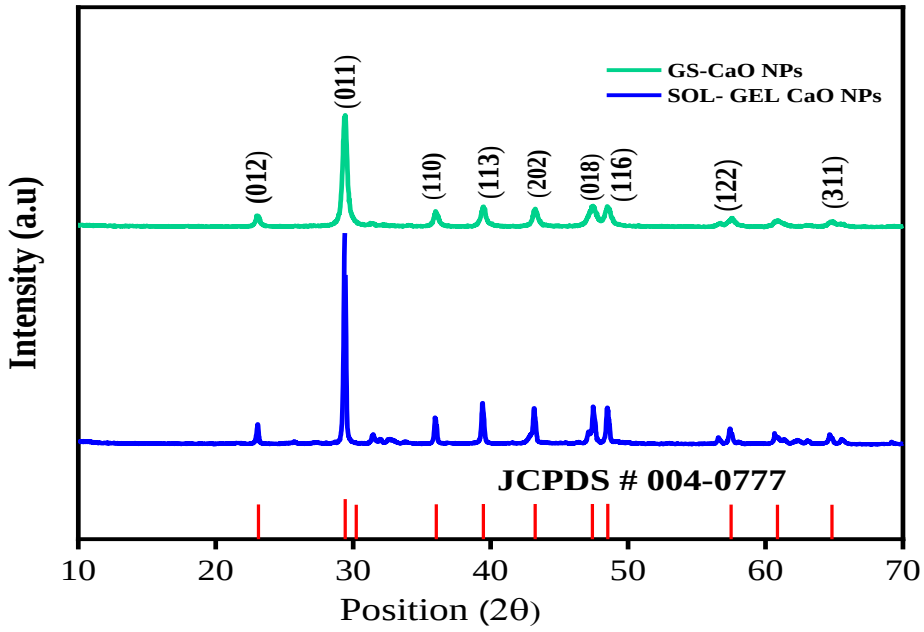

Figure 4.1: XRD patterns of green synthesis CaO NPS a) using Moringa stenopetala leaf extracts b) Sol-gel method

Table 4.1: Variation of crystallite size, micro strain, dislocation density, full width at half maximum, plane spacing of green synthesized calcium oxide nanoparticles using *M. stenopetala* leaf extracts.

S. No	Position(2θ)	FWHM (º)	d(A)	Crystallite Size (nm)	Average crystallite size (nm)	Micro strain ($\times 10^{-4}$)	Dislocation density ($\times 10^{15}$ lines per m^2)
1	23.069	0.3783	3.846	20.566		1.617	2.364
2	29.402	0.4257	3.038	18.046		1.796	3.071
3	36.0378	0.439	2.955	17.203		1.822	3.379
4	39.476	0.4714	2.490	15.855		1.936	3.798
5	43.256	0.4696	2.281	15.719		1.905	4.047

6	47.427	0.7263	1.916	10.010	13.597	2.901	9.978
7	48.538	0.5766	1.875	12.554		2.294	6.344
8	57.520	0.7334	1.602	9.4923		2.805	11.10
9	60.939	0.7403	1.521	9.2453		2.784	11.70
10	64.960	0.9217	1. 437	7.2678		3.393	18.9

Table 4.2: Variation of crystallite size, micro strain, dislocation density, full width at half maximum, plane spacing of Sol-gel synthesized calcium oxide nanoparticles

S. No	Position(2θ)	FWHM (º)	d(A)	Particle Size (nm)	Average crystallite size (nm)	Micro strain ($\times 10^{-4}$)	Dislocation density ($\times$ **10^{14}** lines per m^2)
1	23.046	0.1839	3.850	42.3		7.864	5.59
2	29.390	0.1914	3.034	40.135		8.078	6.2
3	35.991	0.2111	2.84	35.766		8.76	7.82
4	39.428	0.2196	2.493	34.030		9.023	8.635
5	43.173	0.2766	2.093	26.701		11.22	14.0
6	47.482	0.3597	1.913	20.208	29.48	14.37	24.5
7	48.517	0.2678	1.875	27.040		10.65	13.67
8	57.449	0.2889	1.603	24.108		11.05	17.2
9	60.867	0.1969	1.524	34.059		7.26	86.2
10	64.681	0.655	1.439	10.448		24.66	91.6

Table 4.1 clearly shows the calculated and tabulated all crystallite size, micro- strain, and dislocation density using the equations expressed in (2.2 – 2.4) for green synthesis of CaO NPs using Moringa stenopetala leaf extract. The average crystallite of green synthesized CaO NPs computed from all XRD Crystal patterns found to be 13.59 nm. This small crystallite size of CaO NPs leads to reduced internal distortions and the surface crystal defects. From these results, we were understood that as the size of nanoparticles get reduced; the micro-strains and the dislocations density of the crystals were minimized. Similarly, Table 4.2 obviously indicates the observations of important parameters such as crystallite size, micro strain and dislocation densities of Sol- gel synthesized CaO NPs using the Eqn (2.2-2.4). Here also, the average crystallite size of CaO NPs was calculated using all the XRD spectra was found to be 29.48 nm. Generally, using both methods, the minimum surface defects and less impurity of CaO NPs were observed. However, the green method is more preferred and available for the synthesis of the required small size of nanoparticles due to the presence of capping and stabilizing agents during the nanocystals formation.

4.2. Ultraviolet Visible spectroscopy Analysis

Calcium oxide nanoparticles can be analyzed using UV-Vis spectroscopy to determine their optical properties, such as their absorption spectra and band gap energy. In accordance with UV- visible spectra, Figure (4.2a and b) depicts absorption spectra of calcium oxide nanoparticles synthesized using *Moringa stenopetala* leaves extract and sol-gel methods were observed at wavelength intensities 322 and 328 nm respectively. Similar trends were found in the literature (Jadhav et al., 2022; Mazher et al., 2023). Here, CaO NPs synthesized through green synthesis exhibit slightly high absorption peaks as compared to the sol-gel method due to the capability of reducing and stabilizing agents of M. *stenopetala* leaf extract. Also, the absorption of CaO NPs leads to blue shifts with a further increase of the concentration of the sample. More importantly, the band gap energy of CaO NPs can be determined according to Max Planck's equation expressed in (Eqn 2.5)

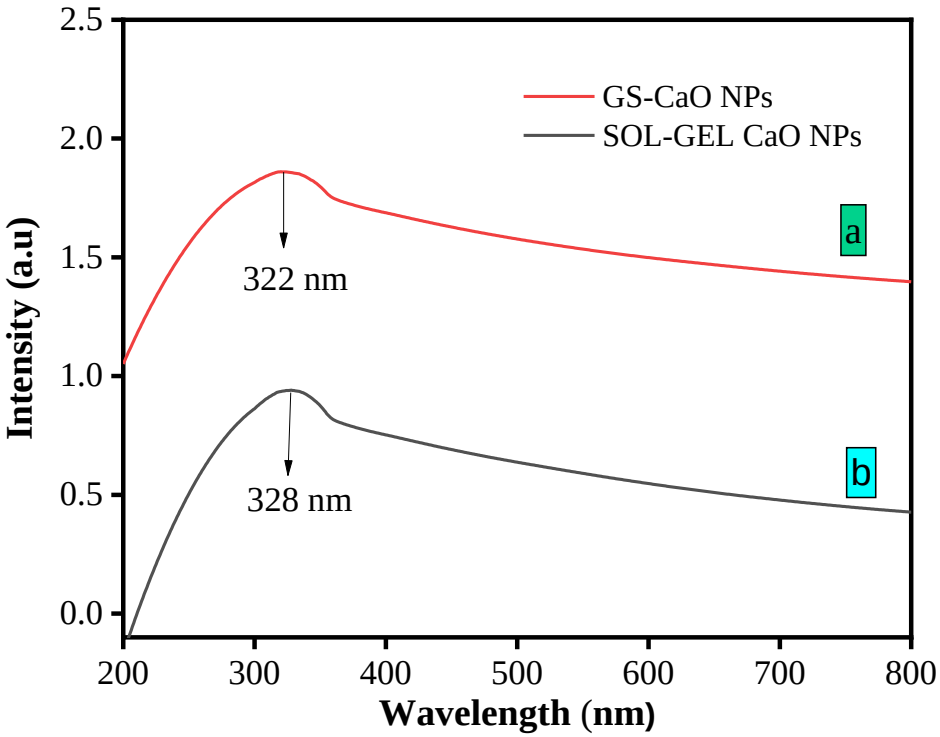

Figure 4.2: UV- visible absorption spectra of CaO NPs a) green synthesized using leaf extracts and b) sol-gel method

Table 4.3: Energy band gap calculated from green synthesized *Moringa stenopetala* and through sol gel method.

S. No	UV-Vis absorption peak spectra in (nm)	Energy band gap (eV)
1	322	3.85
2	328	3.78

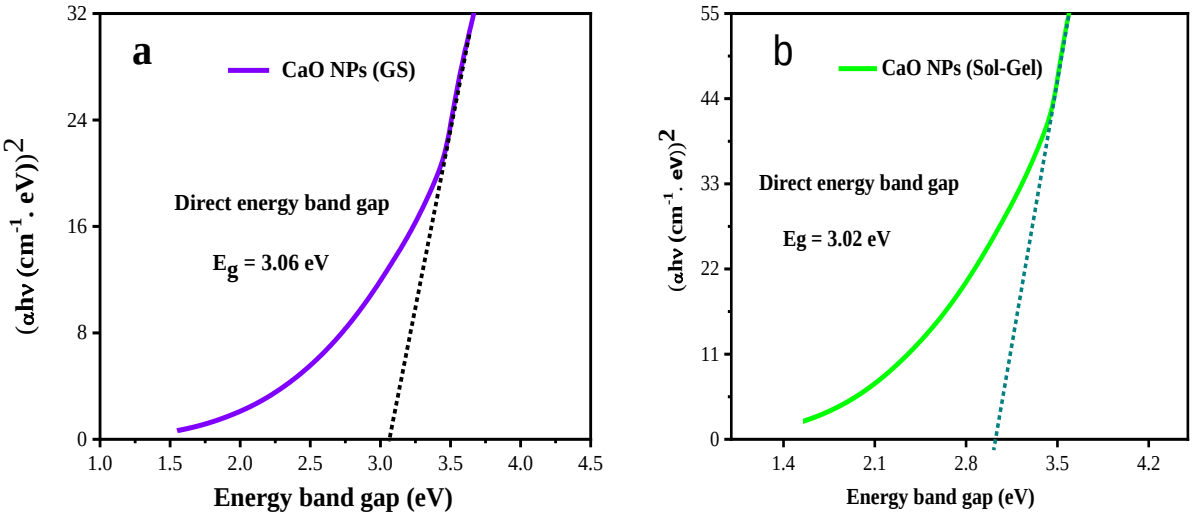

Figure 4.3: Tauc's pilots of drawn (αhϑ)^2 versus optical energy band gap (eV) through a) green synthesized using M. stenopetaala leaf extract b) Sol-gel method

Figure 4.3 above displays the Tauc's plot of green synthesized and sol- gel synthesized calcium oxide nanoparticles. The $(\alpha h\vartheta)^2$ as a function of optical band gap energy showed in the Figure 4.3. In this case, the extrapolation of straight line has drawn from the edge of the graph to x-axis ($\alpha h\vartheta = 0$) and their values were 3.02eV and 3.06 eV for sol-gel synthesized and green synthesized CaO NPs respectively.

4.3. Photoluminescence spectra Analysis

Photoluminescence is a phenomenon where materials emit light after being excited by absorbing photons. Calcium oxide nanoparticles can exhibit photoluminescence when they are excited with light of a specific energy.

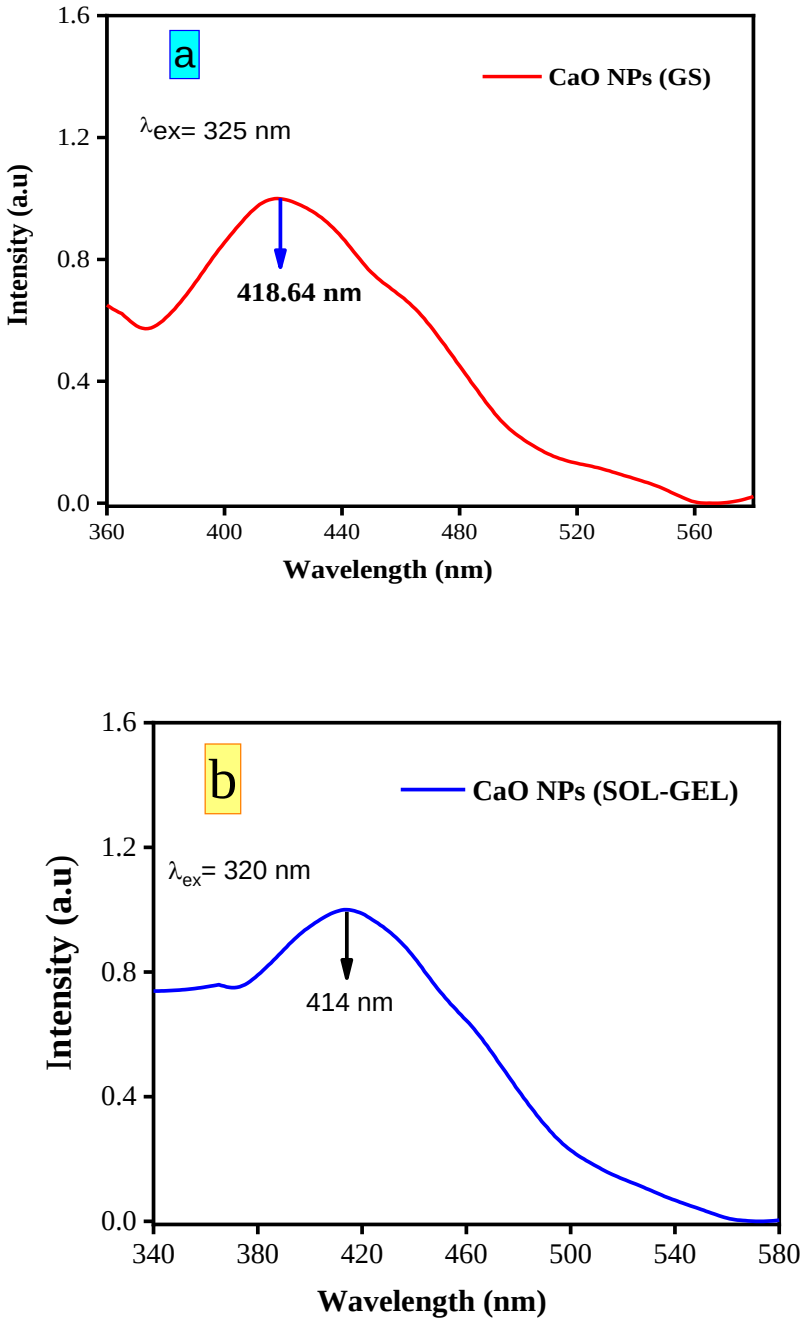

Figure 4.4: The emission spectra of CaO NPs of a) green synthesized using Moringa stenopetala leaf extract b) sol-gel synthesized

Figure (4.4) indicates that the Photoluminescence (PL) emission spectra of calcium oxide nanoparticles (CaO NPs) synthesized using *Moringa stenopetala* leaf extract and sol-gel method were 418.64 nm and 414 nm respectively. Herein, PL spectra of green synthesized CaO NPs using *Moringa stenopetala* leaf extract and sol-gel synthesized CaO NPs can be found by exciting with their excitation wavelength of 325 nm and 320 nm respectively at room temperature as depicted in inset of Figure (4.4). At the excitation of 325 nm, the broad emission peak around 418.64 nm was observed via green synthesized calcium oxide nanoparticles (CaO NPs) which attributed to the radiative recombination of excitons (exciton emission) which means that the electrons made a transition from the conduction to the valence band. Similar observations are also described in the literature (Ikram et al., 2022, Bano & Pillai, 2020).

4.4. Thermogravimetric Analysis

The TGA curve of calcium oxide nanoparticles can provide valuable information about their thermal stability and decomposition behavior. The curve can reveal the temperature at which the nanoparticles start to decompose and the extent of decomposition that occurs. The mass loss can indicate the amount of organic or inorganic material that is present in the sample and the decomposition pathways that occur during heating. In addition to providing information about the thermal stability and decomposition behavior of the nanoparticles, TGA can also be used to study the purity and composition of the sample. The TGA curve can reveal the presence of impurities or contaminants in the sample, as well as the amount of residual solvent or organic material that may be present.

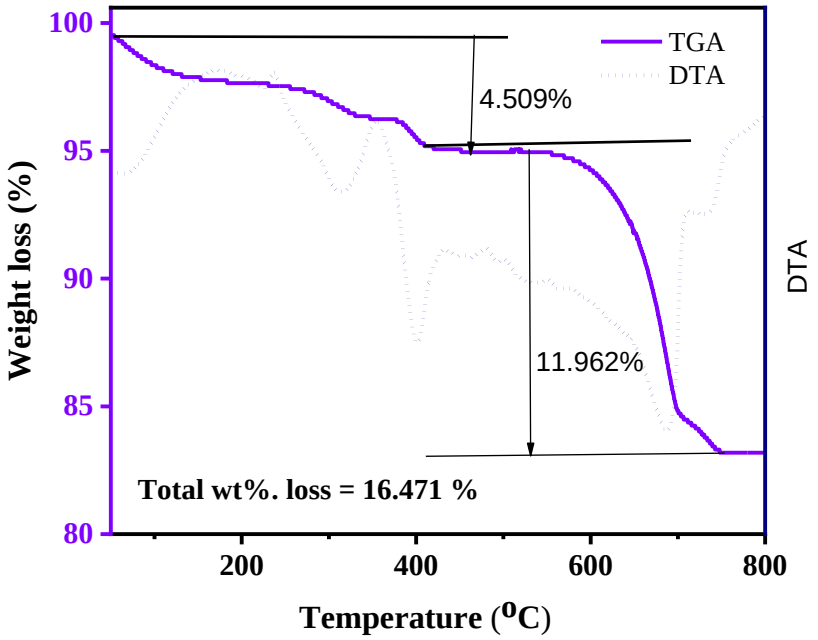

Figure 4.5: Thermogravimetric Analysis (TGA) of sol- gel synthesized CaO NPs

Thermal stability of green synthesized and sol-gel synthesized of calcium oxide (CaO NPs) were determined by TGA and DTA curve heating temperature 25 to 800℃ as depicted in Figure (4.5). As we understand from the TGA curve the decomposition process of sol gel synthesized calcium hydroxide $Ca(OH)_2$ observed in different temperature ranges. The major weight loss stages were visualized. These ranges were 100- 150℃, 250-350℃, 380-413℃, and 560- 750℃. The decomposition of $Ca(OH)_2$ into CaO and water were happened around 400 ℃ (Osuntokun et al., 2018). Based on these observation, the first two couples of temperature indicate that the removal of adsorbent water and some organic material within the sample. The total percentage weight loss of the sample up to 400 ℃ found to be 4.509 %. The second and highest percentage weight loss (11.96%) of $Ca(OH)_2$ were observed between 560℃ and 750℃ which indicate that complete conversion of $Ca(OH)_2$ into calcium oxide nanoparticles (CaO NPs).

4.5. Fourier Transform Infrared Spectroscopy of CaO NPs

The FTIR spectrum of calcium oxide nanoparticles can provide valuable information about the chemical composition and molecular structure of the nanoparticles. The spectrum can reveal the presence of functional groups, such as hydroxyl groups or carbonate groups that are associated with the synthesis or surface modification of the nanoparticles. The spectrum can also reveal the presence of impurities or contaminants in the sample, as well as the crystalline structure of the nanoparticles.

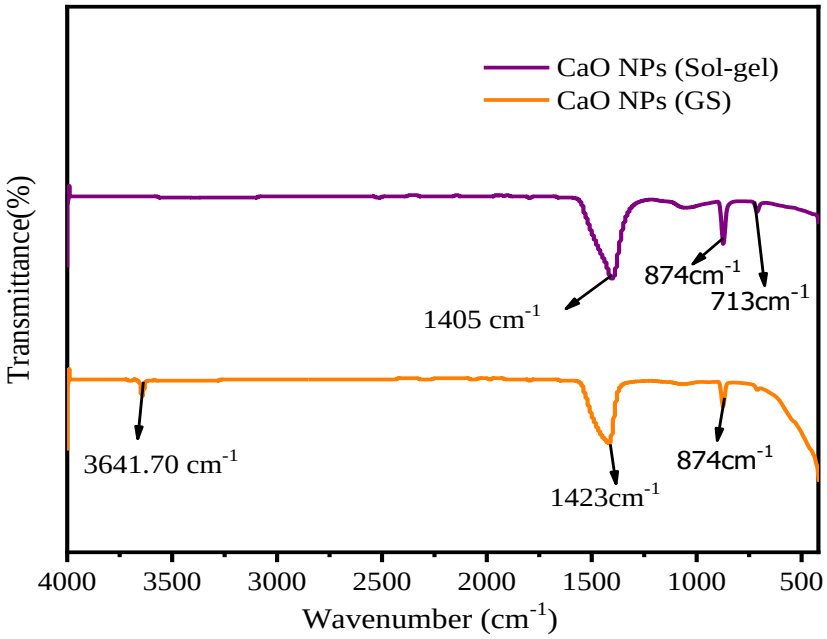

Figure 4.6: Fourier Transform Infrared Spectroscopy of CaO NPs

FTIR analysis was carried out to determine the interaction between both green synthesized and sol gel methods of forming CaO NPs and the phytochemical components of *Moringa stenopetala* plant extract. As we have seen in the Figure (4.6), FTIR spectra of green synthesized and sol gel synthesized calcium oxide nanoparticles and with their correspondence wave numbers were formed. On the spectra of green synthesized of calcined at 500 ℃ leads to form three important spectra bands at 1405 cm^{-1}, 874 cm^{-1}, and 713 cm^{-1}. The peaks at 1400 and 877 cm^{-1} correspond to the C−O bond associated with the carbonation of CaO nanostructures. The band at 712 cm^{-1} shows the Ca−O bonds

confirming the CaO NP formation (Ikram et al., 2022). A broad absorption band in the range of between 3650 and 3250 cm^{-1}, indicating hydrogen bond (Nandiyanto et al., 2019). The occurrence of O-H stretching at 3641 cm^{-1} is due to the absorption of moisture present in the atmosphere during the pellet preparation process (Sarathy, 2018). The broad bands that occurred around the 1405 and 1423 cm^{-1} exhibit the carbonation of CaO NPs.

4.6. Scanning Electron Microscope Analysis

Scanning electron microscopy (SEM) was another and important technique used to analyze the surface morphology of the synthesized nanoparticles.

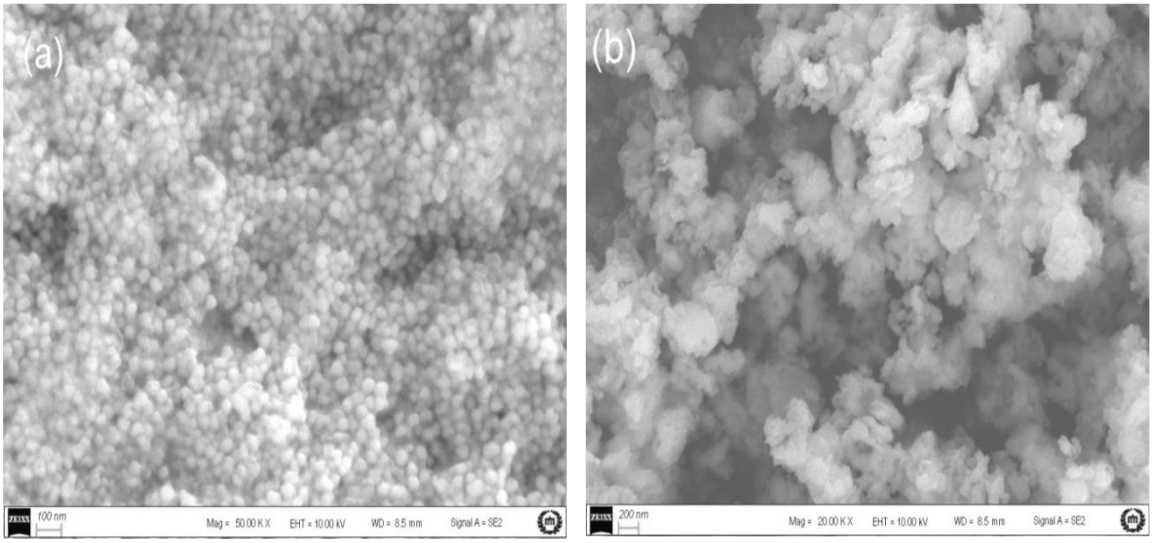

Figure 4.7: Scanning electron microscope images of CaO NPs a) green synthesized using M. stenopetala leaf extract b) sol-gel method

In the case of our study, the size and shape of both green synthesized and sol-gel method synthesized CaO NPs were screened and identified. Figure 4.7 shows the small spherical morphology and the cubic phase of CaO NPs were observed for green synthesized using *Moringa stenopetala* leaf extract and the sol-gel method respectively. The average particle sizes determined from the SEM morphology were 24.15 nm for green synthesized calcium oxide nanoparticles and 90- 110 nm for the sol gel method synthesis. These crystallite size values were analyzed by using IMAGE J SOFTWARE. The SEM image of sol-gel synthesized CaO NPs consistent with results obtained from the sol gel synthesized of CaO NPs using chicken eggshells (Habte et al., 2019).

4.7. Antibacterial Activities Assay

In these studies, the CaO NPs were performed on the two Gram-positive bacteria (*Staphylococcus aureus, S. aureus* and *Streptococcus pneumonia, S. pyognes*) and Gram-negative bacteria (*Escherichia coli, E. coli, Pseudomonas, aeruginosa, P. aeruginosa*) by disk diffusion methods. In this manner, the antibacterial of CaO NPs synthesized by green synthesized using *Moringa stenopetala* leaf extract and synthesized through sol-gel method and their mixture were conducted on each type of bacterial strain. Here, the CaO NPs synthesized via green synthesis using *M. stenopetala* and sol-gel method and also their equal mixture (composites) against four types of bacterial strains are displayed in the following (Fig. 4.8- 4.10). The antibacterial activity of green synthesized CaO nanoparticles with dopant *Mentha pipertia* and synthesized via direct precipitation has been stated in related literature (Kumar et al., 2021; Srimathi Pasupathy & Manivannan Rajamanickam, 2019).

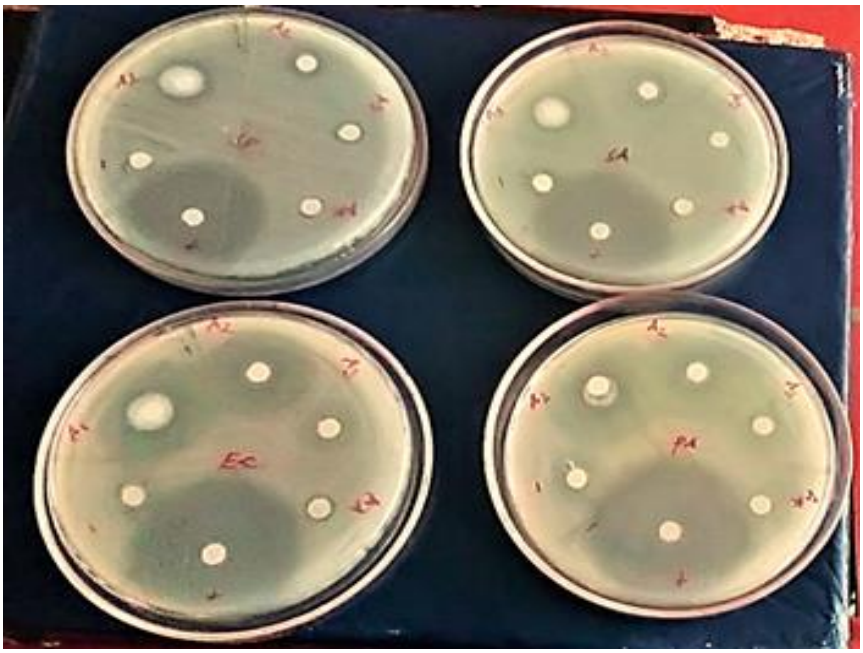

Figure 4.8: Antibacterial activity of calcium oxide synthesized via green synthesized using Moringa stenopetala leaf extract against (E. coli, P. aeruginosa, S. aureus, S. pyogenes)

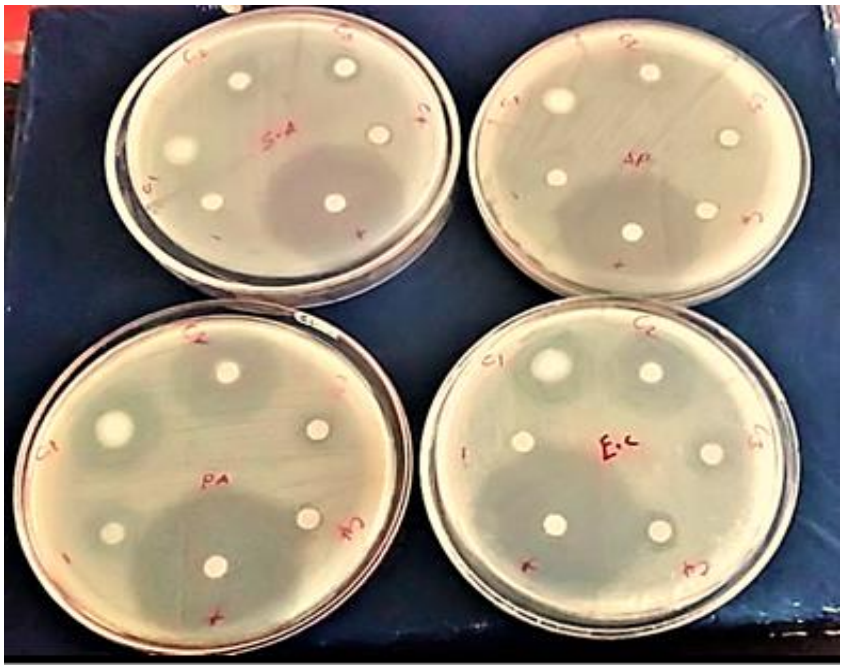

Figure 4.9: Antibacterial activity of calcium oxide synthesized sol gel method against (E. coli, P. aeruginosa, S. aureus, S. pyogenes)

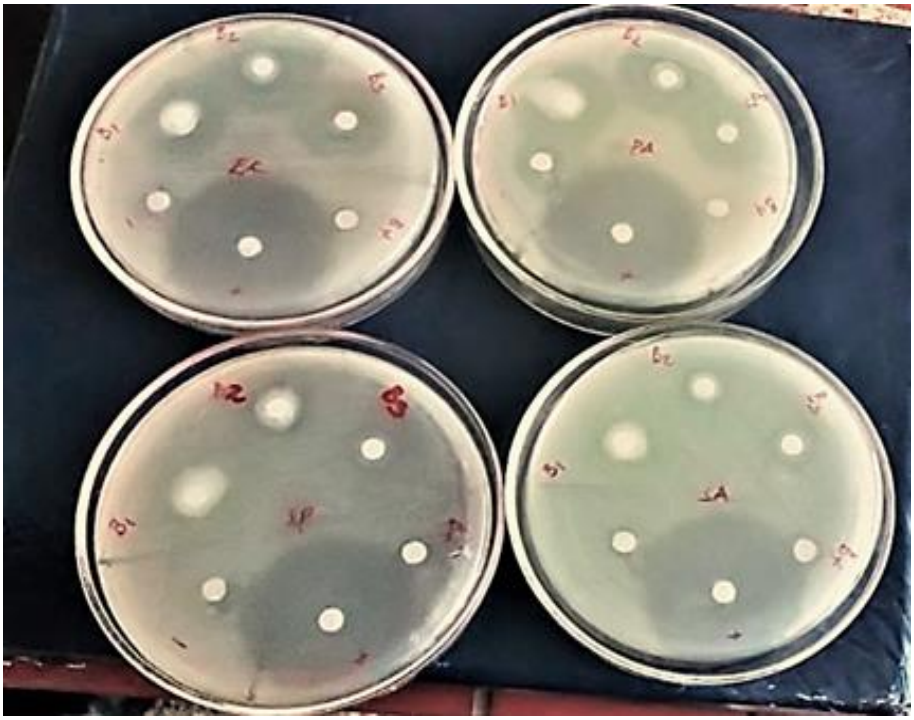

Figure 4.10: Antibacterial activity of calcium oxide synthesized from both green synthesized and sol gel method against (E. coli, P. aeruginosa, S. aureus, S. pyogenes)

The antibacterial activity of green synthesized Calcium oxide (CaO) nanoparticles using *Moringa stenopetala* and via sol gel method against typical bacterial strains Gram -ve (*E. coli, P. aeruginosa*) and Gram +ve bacteria (*S. aureus, S. pyogenes*) were recorded and described in the table (4.4-4.6). The screening of an inhibition zone indicates that the mechanisms of the bactericidal performance of CaO NPs exhibits destroying of cell membrane due to small size and large surface area as well as the creation more reactive oxygen species (ROS) which can cause the cell death of target pathogens. Surprisingly, the dimensions of zone inhibition were varied in accordance with the kinds of pathogen species, the concentration and the synthesis methods of calcium oxide nanoparticles (Roy et al., 2013). In this work, the important mechanism was the release of Ca^{+2} from calcium oxide nanoparticles transferred into the cultured bacterial strains and makes the generation of radicals such as superoxide ion (O_2^-), hydroxyl ion (OH^-) and peroxide ion (H_2O_2). The first two negative radicals weak to enter the bacterial cell membrane cause death because of their negative charges. Peroxide ions are highly reactive and easily penetrate the cell membrane and lead to interrupt the bacterial DNA replication.

Table 4.4: Zones of inhibition of green synthesized CaO NPs using *Moringa stenopetala* with Variety of bacterial strains of a gram (+ve) and gram (-ve) bacteria with concentrations of 6.25 mg/mL, 12.5 mg/mL, 25 mg/mL, and 50 mg/mL.

Samples	Concentrat-ion (mg/ml)	Mean zones of inhibition in diameter (mm)			
		Types of Bacterial Strains (Gram +ve and Gram –ve)			
GS- CaO NPs		E. coli	P. aeruginosa	S. aureus	S. pyogenes
	50	24.1±0.764	15.5±0.288	14.160.763	15.83±0.289
	25	22.83±1.04	14±1.00	12.15±0.764	12.67 ± 1.53
	12.5	12.0±1.00	9.67±2.082	10.5±0.5	9.16±0.764
	6.25	8.16±0.763	7.33±0.577	7.33 ± 0.577	7.5±0.50

The different concentration green synthesized CaO NPs using *Moringa stenopetala* leaf extracts was subjected to antimicrobial activity and the results were observed as tabulated in Table 4.4. Ciproflocaxin antibiotic standard were used as positive control. In this sense, the four concentration of MS- CaO NPs 6.25, 12,5, 25 and 50mg/mL were applied by using disk diffusion method on the four the various bacterial strains and showed the good antibacterial activity on each strain. More importantly, increasing the concentration of MS-CaO NPs (as we move bottom to the top of each column of above table) makes the activity of nanoparticles significantly increases. These can be ensured in comparable with the ciprofloxacin (positive control).

However, the mean diameter of their inhibition investigated was different regarding gram-positive bacteria (S. aureus, S. pyogens) and gram-negative bacteria (*E. coli. P.aeruginosa*). The size of inhibition within the gram negative bacteria became high in comparison with gram-positive bacteria due to the susceptibility of gram-negative bacteria to green synthesized nanoparticles CaO using MS leaf extract. The grams negative bacteria (*E. coli. P, aeruginosa*) possess a single layer of cell membrane and are easy for nanoparticle entrance. Therefore, the maximum inhibition zones *Moringa stenopetala*-CaO NPs was observed with the concentration of 50mg/mL were 24.1 ± 0.764mm, 15.5 ± 0.288 mm 14.16 ± 0.763 mm, 15.83 ± 0.289 mm and the minimum inhibition zones were also recorded within the 6.25 mg/ml concentration 8.16 ± 0.763mm, 7.33 ± 0.577 mm, 7.33 ± 0.577 mm, 7.5 ± 0.50mm CaO NPs for the strains of *E. coli, P.aeruginosa, S. aureus and, S. pyogenes* respectively. The other inhibition zones of nanoparticles moderately effective for both gram negative and gram positive bacteria. These practical antibacterial activity observations of CaO NPs on various kinds of strains were more meaningful as compared with 1mg/ mL of Ciprofloxacin antibiotic (positive control) by its inhibition zone ranges between 30 and 31 mm.

*Mean values of three triplicates ± standard deviation

Table 4.5: Zones of inhibition of sol -gel synthesized CaO NPs using *Moringa stenopetala* with several of bacterial strains of a gram (+ve) and gram (-ve) bacteria with concentrations of 6.25 mg/mL, 12.5 mg/mL, 25 mg/mL, and 50 mg/mL.

Samples	Concentrat-ion (mg/ml)	Mean zones of inhibition in diameter (mm)			
		Types of Bacterial Strains (Gram +ve and Gram –ve)			
S -gel- CaO NPs		E. coli	P. aeruginosa	S. aureus	S. pyogenes
	50	20.75±1.56	19.6±2.460	15.67±0.69	17.3±3.055
	25	15.33±1.53	18.3±0.577	12.3±0.50	14.67±1.155
	12.5	10.58 ± 0.72	11.66±1.527	10.08±0.127	8.42±0.52
	6.25	9.45±0.507	9.67±2.08	9.07 ± 0.35	7.25 ± 0.433

The sol-gel synthesized calcium oxide nanoparticles (CaO NPs) was applied to the antimicrobial activity and the results were investigated as tabulated in (Table 4.5). This can be done by using the disk diffusion method by taking four various concentrations of CaO NPs and made exposed with the human pathogenic bacteria which are gram -negative (E. coli, *P. aeruginosa*) and gram-positive (*S. aureus, S. pyogenes*). Like in MS- CaO NPs, the concentration of the synthesized CaO nanoparticles were clearly affects the size inhibition zone of bacterial cells as well as the vulnerability of gram negative bacteria to the CaO NPs. The ciproflocaxin antibiotic standard applied as positive control parallel with the chosen concentration of nanoparticles and it showed the largest inhibition zone of the strains. Although the microbial activity of CaO NPs of the sol-gel method synthesized was good, it exhibited moderate inhibition zone in comparison with green synthesized CaO NPs using *Moringa stenopetala* leaf extract due to the role of *Moringa stenopetala* for antibacterial activity. In these finding, the maximum mean diameter inhibition were obtained for 50mg/mL of CaO with the respective zones of 20.75±1.56 mm,

19.6±2.460 mm , 15.67±0.69 mm, 17.3±3.055 mm and also measured relatively minimum inhibition zones within the concentration of 6.25 mg/ ml which corresponds inhibition zones of 9.45±0.507 mm, 9.67±2.08 mm , 9.07 ±0,35 mm, 7.25 ± 0.433 mm *E. coli*, *P. aeruginosa*, *S. aureus*, and *S. pyogenes* respectively. The ciprofloxacin antibiotic standard measured the inhibition zones between 33 and 34 mm.

Table 4.6: Zones of inhibition of CaO NPs synthesized both green method using *Moringa stenopetala* and sol-gel method with several of bacterial strains of a gram (+ve) and gram (-ve) bacteria with concentrations of 6.25 mg/mL, 12.5 mg/mL, 25 mg/mL and 50mg/mL.

Samples	Concentrat-ion (mg/ml)	Mean zones of inhibition in diameter (mm)			
		Types of Bacterial Strains (Gram +ve and Gram –ve)			
GS and Sol-gel CaO NPs		E. coli	P. aeruginosa	S. aureus	S. pyogenes
	50	23.08±0.946	22.75±0.926	14.42±0.52	23.58±1.506
	25	16.17±0.764	25.08±0.877	12.58±0.520	15.58±0.520
	12.5	13.58±0.52	12.78±1.068	12.12±1.02	13.32±0.592
	6.25	9.08±0.878	9.45±0.507	7.75±1.09	9.11±0.83

The calcium Oxide nanoparticles synthesized through both the green synthesis method and the Sol-gel method were subjected to the antimicrobial activity and the results were collected. The equal mixtures of the two (composites) samples with the concentration of 50mg/mL showed 23.08±0.946 mm and 22.75±0.926 mm zone of inhibition on the *Escherichia coli*, and *P. aeruginosa*, gram-negative bacteria respectively. And also, zone

of inhibition on *Staphylococcus aureus*, and S. pyogenes, gram positive bacteria were 14.42±0.52 *mm* and 23.58±1.506 mm respectively. Thus composites of the two different synthesized CaO NPs showed highly active and measures high inhibition zones as related with the individual synthesized CaO NPs. That is, due to the enhancement of the composition, optical and the electrical properties which helps to produce the calcium ion (Ca^{2+}) and create the reactive oxygen species (ROS). Even at the initial concentration of 6.25 mg/mL it showed effective and clear inhibition zones of 9.08±0.878 mm, 9.45±0.507 mm,7.75±1.09 mm, and 9.11±0.83 mm for *E. coli P. aeruginosa S. aureus S. pyogenes* respectively. The ciprofloxacin also revealed the highest inhibition zones of each bacterial cell where their values lie between 33 and 34 mm.

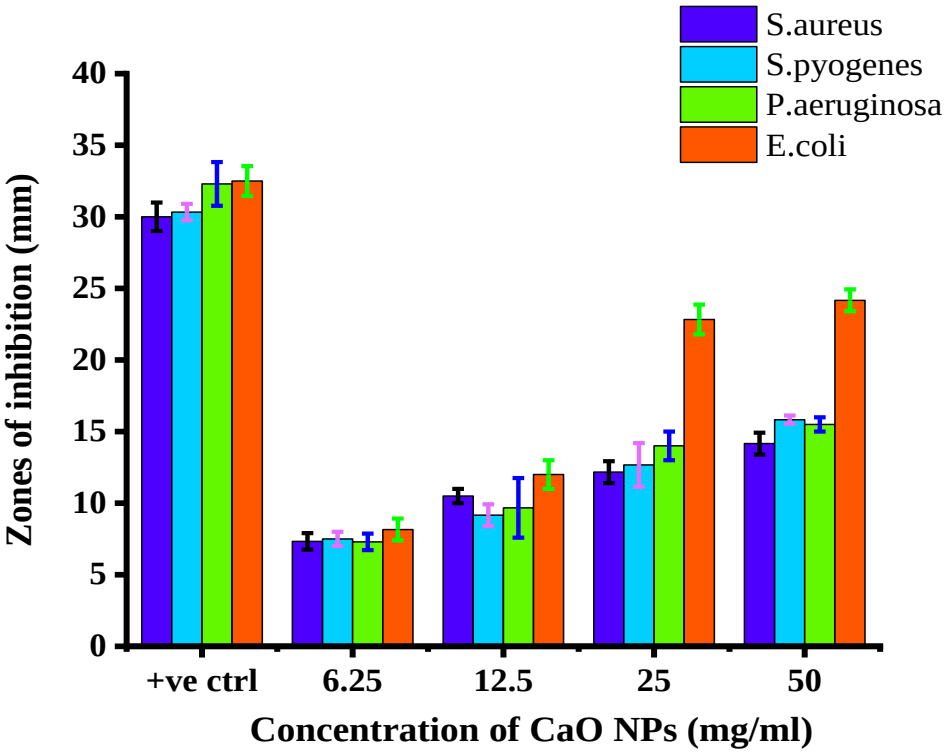

Figure 4.11: The size of Zones of inhibition formed around each disk versus the different concentration of green synthesized of CaO NPs using M. stenopetala leaf extract against four selective bacterial strains of Gram positive and gram negative bacteria

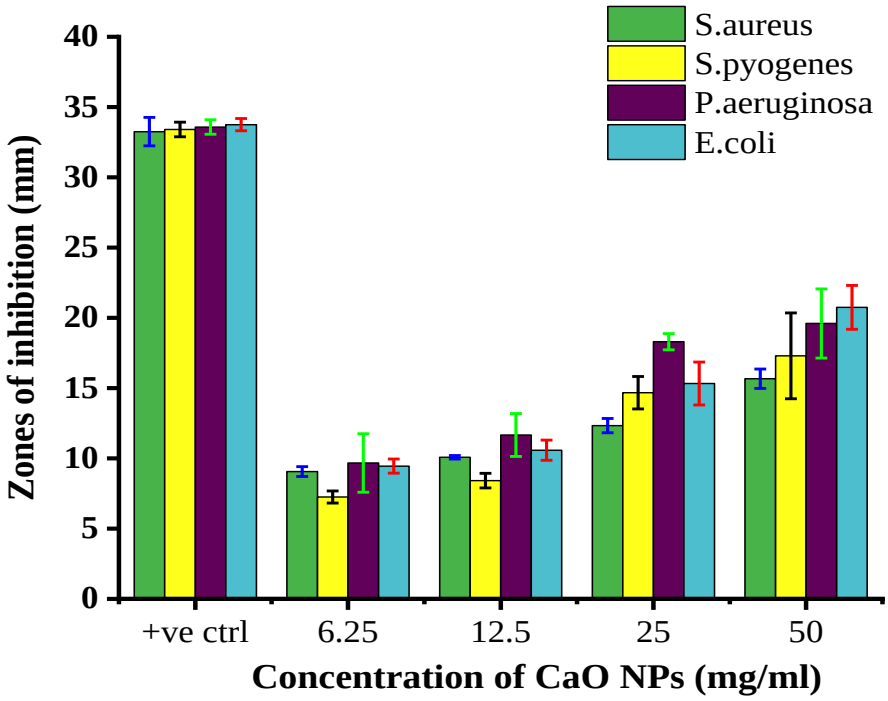

Figure 4;7: The size of Zones of inhibition formed around each disk versus the different concentration of sol-gel synthesized of CaO NPs against four selective bacterial strains of Gram-positive and gram-negative bacteria

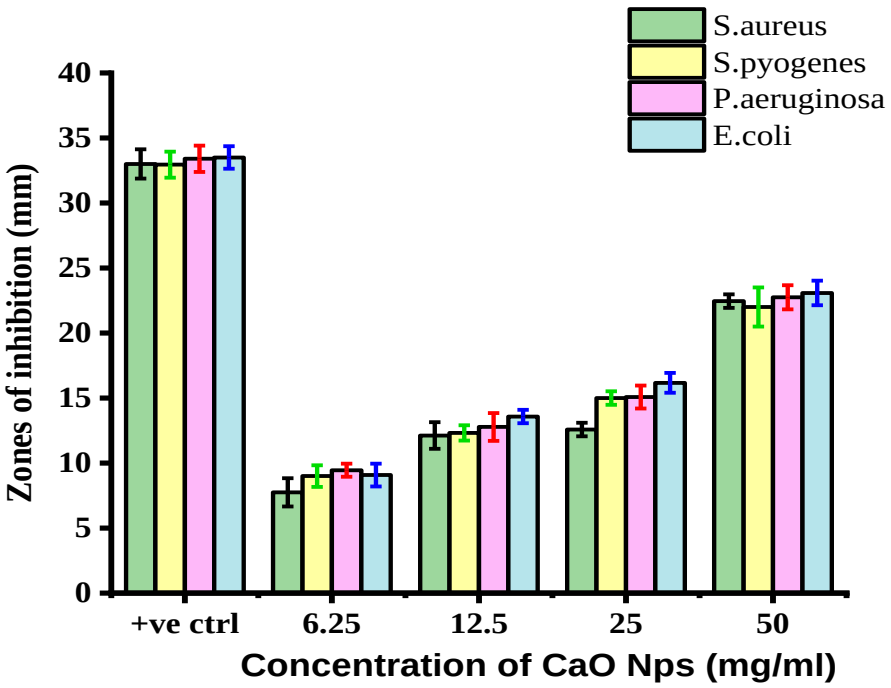

Figure 4.13: The size of Zones of inhibition formed around each disk versus the different concentration of both green synthesized of CaO NPs using M. stenopetala leaf extract and sol-gel method against four selective bacterial strains of Gram-positive and gram-negative

CHAPTER 5 - CONCLUSION AND RECOMMENDATIONS

5.1. Conclusion

In this study, the Calcium Oxide nanoparticles (CaO NPs) were synthesized through green synthesis method using *Moringa stenopetala* leaf extract and sol- gel method by using calcium tetrahydrate as the precursor and Sodium hydroxide as PH controller and the precipitating agent in the synthesis conditions. The synthesized CaO NPs samples were then characterized by spectroscopic techniques like X-ray diffractometer (XRD), UV-Visible Spectroscopy (UV-Vis), Photoluminescence (PL), Thermogravimetric Analysis (TGA), Fourier Transform Infrared (FTIR) Spectroscopy and Scanning Electron microscope (SEM). The XRD showed that the green synthesis of CaO NPs using *Moringa stenopetala* leaf extract and sol-gel synthesized CaO NPs were possessed average crystallite size 13.59 nm and 29.48 nm respectively. These indicate that CaO NPs exhibit high crystalline nature. Based on UV-Vis Spectroscopy analaysis, the energy band gap of the green synthesized using *Moringa stenopetala* leaf extracts and the sol-gel method synthesized CaO NPs were determined. These results revealed that the energy band gap of the green synthesized CaO NPs became wider i.e. the realization of the wide band gap energy of CaO NPs. It also found that, from photoluminescence (PL) analysis of the green synthesized (MS-CaO NPs) and sol- gel method of CaO NPs showed the UV- emission and near band edge emission respectively. By using Thermogravimetric Analysis, it can be observed that the initial decomposition process of CaO NPs occurred between 100 ℃ up to 400 ℃. These temperature ranges indicate that the removal of adsorbent water within sample surface. Around the 400 ℃, the Calcium hydroxide was transformed into CaO and water in sample contents. And also, the complete conversion of $Ca(OH)_2$ into CaO occurred between 550 ℃ and 750 ℃.

The FT-IR Spectroscopy revealed the existence of functional groups attached to green synthesized CaO NPs and Sol-gel method synthesized CaO NPs like the hydroxyl group (OH) and which further confirmed the Ca-O bond formation. In Scanning electron microscope analysis, the green synthesized CaO NPs exhibited spherical shapes and the respective average particles size were 24.15 nm and scanned the cubic phase of CaO NPs from the sol-gel method synthesis and their average particles size lie in the range of 90 – 110 nm. The antibacterial assay of green synthesized using Moringa stenopetala leaf extract and sol-gel synthesized CaO NPs against two gram-positive bacterial strains (S.

aureus, S. pyogenes) two gram-negative bacterial strains *(E. coli*, *P. aeruginosa*) were carried out by using disk diffusion methods. These observations justified the susceptibility of gram-negative bacterial strains to the green synthesized using *Moringa stenopetala* leaf extracts and sol-gel method synthesis of CaO NPs. Additionally, with the further increase of the concentration of CaO NPs results in more efficacy of antimicrobial activity.

5.2. Recommendations

The green synthesis method for alkaline earth metals (AEM) has been the most interesting research area in future prospective. Further studying and more understanding of the green synthesis method on alkaline earth metals such Ca, Mg, and so forth, are so important for multifunctional applications like in biomedical, catalysis, biodiesel, optoelectronics, environmental remediation and antimicrobial activities.

In this work, mainly the concentration of the green synthesized of CaO NPs using *Moringa stenopetala* increases its capability shows more efficiency on the bacterial activity as compared with sol-gel method synthesis. Therefore, other interested researchers can be expand the knowledge by working on this area and will extend their thought beyond the obtained results.

REFERENCES

Alobaidi, Y. M., Ali, M. M., & Mohammed, A. M. (2022). Synthesis of Calcium Oxide Nanoparticles from Waste Eggshell by Thermal Decomposition and their Applications. *Jordan Journal of Biological Sciences*, *15*(2), 269–274.

Anowar Hossain, M. (2021). Adaptive Camouflage Textiles with Thermochromic Colorant and Liquid Crystal for Multidimensional Combat Background, a Technical Approach for Advancement in Defence Protection. *American Journal of Materials Engineering and Technology*, *9*(1), 31–47.

Atchudan, R., Perumal, S., Joo, J., & Lee, Y. R. (2022). Synthesis and Characterization of Monodispersed Spherical Calcium Oxide and Calcium Carbonate Nanoparticles via Simple Pyrolysis. *Nanomaterials*, *12*(14).

Azam, A., Ahmed, A. S., Oves, M., Khan, M. S., Habib, S. S., & Memic, A. (2012). Antimicrobial activity of metal oxide nanoparticles against Gram-positive and Gram-negative bacteria: A comparative study. *International Journal of Nanomedicine*, *7*, 6003–6009.

Bano, S., & Pillai, S. (2020). Green synthesis of calcium oxide nanoparticles at different calcination temperatures. *World Journal of Science, Technology and Sustainable Development*, *17*(3), 283–295.

Butt, A. R., Ejaz, S., Baron, J. C., Ikram, M., & Ali, S. (2015). CaO nanoparticles as a potential drug delivery agent for biomedical applications. *Digest Journal of Nanomaterials and Biostructures*, *10*(3), 799–809.

Chemistry, A. (2019). *Preparation and Characterization Nanoparticle Calcium Oxide from Snakehead Fish Bone using Ball Milling Method*. 111–115.

Chinthakuntla, A., Thatikayala, D., Rao, K. V., Chakra, C. S., & Kumar, M. K. (2015). Calcium Oxide Nano Particles Synthesized From Chicken Egg Shells by Physical Method. *International Conference on Emerging Technologies in Mechanical Sciences*, *December*, 72–75.

Demissie, M. G., Sabir, F. K., Edossa, G. D., & Gonfa, B. A. (2020). Synthesis of Zinc Oxide Nanoparticles Using Leaf Extract of Lippia adoensis (Koseret) and Evaluation of Its Antibacterial Activity. *Journal of Chemistry*, *2020*.

Duguma, H. T., Azene, M., Chameno, G., & Haile, M. (2022). Antimicrobial properties of Moringa Stenopetala seed oil. *African Journal of Microbiology Research*, *16*(11), 343–348.

Eram, R., Kumari, P., Panda, P., Singh, S., Sarkar, B., Mallick, M., & Verma, S. (2021). Cellular Investigations on Mechanistic Biocompatibility of Green Synthesized Calcium Oxide Nanoparticles with Danio rerio. *Journal of Nanotheranostics*, *2*(1).

Gurav, V. L., Samant, R. A., Manjare, S. B., Patil, U. K., Solkar, S. R., & Moghe, S. S. (2020). Asian Journal of Nanoscience and Materials Biosynthesis of calcium oxide nanoparticles using Ocimum sanctum (Tulsi) leaf extracts and screening its antimicrobial activity. *Asian Journal of Nanoscience and Materials*, *3*, 415639.

Habte, L., Shiferaw, N., Mulatu, D., & Thenepalli, T. (n.d.). *Synthesis of Nano-Calcium Oxide from Waste Eggshell by Sol-Gel Method*. 1–10.

Hadi, M., Mahboobeh, M., & Behjat, Z. (2022). Facile green synthesis of CaO NPs using the Crataegus pontica C . Koch extract for photo - degradation of MB dye. *Environmental Science and Pollution Research*, 54688–54697.

Hadi, M., & Mehdi, M. (2023). *International Journal of New Chemistry Facile and Eco-Friendly Method for Synthesis of Calcium Oxide Nanoparticles Utilizing Pistacia Atlanica Leaf Extracts and Its Characterization*. *10*(1), 81–88.

Hadis, M., Gebreyohannes, Y., & Gemeda, N. (2020). Potential therapeutic uses of Moringa stenopetala : a scoping review . *Journal of Global Health Science*, *2*(2).

Hoseinzadeh, E., Makhdoumi, P.,P. T.-C. drug, & 2017). A review on nano-antimicrobials.

Ikram, M., Khan, A. M., Haider, A., Haider, J., Naz, S., Ul-hamid, A., Shahzadi, A., Nabgan, W., Shujah, T., Shahzadi, I., & Ali, S. (2022). *Facile Synthesis of La- and Chitosan-Doped CaO Nanoparticles and Their Evaluation for Catalytic and Antimicrobial Potential with Molecular Docking Studies*.

Jadhav, V., Bhagare, A., Wahab, S., Lokhande, D., Vaidya, C., Dhayagude, A., Khalid, M., Aher, J., Mezni, A., & Dutta, M. (2022). Green Synthesized Calcium Oxide Nanoparticles (CaO NPs) Using Leaves Aqueous Extract of Moringa oleifera and Evaluation of Their Antibacterial Activities. *Journal of Nanomaterials*, *2022*, 1–7.

Jubu, P. R., & Muhammad, A. (2022). *Considerations About the Determination of Optical Bandgap from Diffuse Reflectance Spectroscopy Using the Tauc Plot*. 1–19.

Kebede Urge, S., Tiruneh Dibaba, S., & Belay Gemta, A. (2023). Green Synthesis Method of ZnO Nanoparticles using Extracts of Zingiber officinale and Garlic Bulb (Allium sativum) and Their Synergetic Effect for Antibacterial Activities. *Journal of Nanomaterials*, *2023*.

Kumar, M., & Ranjan, R. (2022). *XRD Analysis for Characterization of Green Nanoparticles : A Mini Review XRD Analysis for Characterization of Green Nanoparticles : 10*, 2–5.

Kumar, S., Sharma, V., Pradhan, J. K., Sharma, S. K., Singh, P., & Sharma, J. K. (2021a). Structural, optical and antibacterial response of CaO nanoparticles synthesized via direct precipitation technique. *Nano Biomedicine and Engineering*, *13*(2), 172–178.

Kumar, S., Sharma, V., Pradhan, J. K., Sharma, S. K., Singh, P., & Sharma, J. K. (2021). Structural, optical and antibacterial response of CaO nanoparticles synthesized via direct precipitation technique. *Nano Biomedicine and Engineering*, *13*(2), 172–178.

Marasini, B., Pagar, T., Ghotekar, S., Pansambal, S., Oza, R., & Marasini, B. P. (2020). Facile Plant Extract Mediated Eco-Benevolent Synthesis and Recent Applications of CaO-NPs. *Journal of Chemical Reviews*, *2*(3), 201–210.

Mazher, M., Ishtiaq, M., Hamid, B., Haq, S. M., Mazhar, A., Bashir, F., Mazhar, M., Mahmoud, E. A., Casini, R., Alataway, A., Dewidar, A. Z., & Elansary, H. O. (2023). *Biosynthesis and Characterization of Calcium Oxide Nanoparticles from Citrullus colocynthis Fruit Extracts ;* 1–21.

Mushtaq, M., Hassan, S. M., & Mughal, S. S. (2022). Synthesis, Characterization and Biological Approach of Nano Oxides of Calcium by Piper nigrum. *American Journal of .*., *10*(4), 79–88.

Nandiyanto, A. B. D., Oktiani, R., & Ragadhita, R. (2019). How to read and interpret ftir spectroscope of organic material. *Indonesian Journal of Science and Technology*, *4*(1), 97–118. https://doi.org/10.17509/ijost.v4i1.15806

Naseem, T., & Durrani, T. (2021). The role of some important metal oxide nanoparticles for wastewater and antibacterial applications: A review. *Environmental Chemistry and Ecotoxicology*, *3*, 59–75.

Nuryantini, A. Y., Sundari, C. D. D., Halimahtussa'diah, H., & Nuryadin, B. W. (2019). Synthesis and Characterization of Calcium Oxide Nanoparticles from Duck Eggshells using Ball Milling Methods. *Jurnal Kimia Valensi*, *5*(2), 231–135.

Osuntokun, J., Onwudiwe, D. C., & Ebenso, E. E. (2018). Aqueous extract of broccoli mediated synthesis of CaO nanoparticles and its application in the photocatalytic degradation of bromocrescol green. *IET Nanobiotechnology*, *12*(7), 888–894.

Ramli, M., Rossani, R. B., Nadia, Y., Banta Darmawan, T., Febriani, Saiful, & Ismail, Y. S. (2019). Nanoparticle fabrication of calcium oxide (CaO) mediated by the extract of red dragon fruit peels (Hylocereus Polyrhizus) and its application as inorganic-anti-microorganism materials. *IOP Conference Series: Materials Science and Engineering*, *509*(1), 13–18.

Ramli, M., Rossani, R. B., Nadia, Y., & Darmawan, T. B. (n.d.). *Nanoparticle fabrication of calcium oxide (CaO) mediated by the extract of red dragon fruit peels (Hylocereus Polyrhizus) and its application as inorganic – anti-microorganism materials Nanoparticle fabrication of calcium oxide (CaO) mediated by the*. 13–18.

Ramola, B., & Joshi, N. C. (2019). Green Synthesis, Characterisations and Antimicrobial Activities of CaO Nanoparticles. *Oriental Journal of Chemistry*, *35*(3), 1154–1157.

Reports, N. (2020). *Facile Synthesis of Calcium Oxide Nanoparticles from the Carica Papaya Leaf Extract with the Significantly Enhanced Antibacterial Activity*. *3*(3), 1–9.

Roy, A., & Bhattacharya, J. (2011). Microwave-assisted synthesis and characterization of CaO nanoparticles. *International Journal of Nanoscience*, *10*(3), 413–418.

Roy, A., Gauri, S. S., Bhattacharya, M., & Bhattacharya, J. (2013). Antimicrobial activity of CaO nanoparticles. *Journal of Biomedical Nanotechnology*, *9*(9), 1570–1578.

Sarathy, V. P. (2018). *Research Article Biomedical Applications of Calcium Oxide Nanoparticles - A Spectroscopic Study*. *49*(19), 121–125.

Shakhatreh, M. A. K., Al-Smadi, M. L., Khabour, O. F., Shuaibu, F. A., Hussein, E. I., & Alzoubi, K. H. (2016). Study of the antibacterial and antifungal activities of synthetic benzyl bromides, ketones, and corresponding chalcone derivatives. *Drug Design, Development and Therapy*, *10*, 3653–3660.

Singh, J., Dutta, T., Kim, K. H., Rawat, M., Samddar, P., & Kumar, P. (2018). "Green" synthesis of metals and their oxide nanoparticles: Applications for environmental remediation. *Journal of Nanobiotechnology*, *16*(1), 1–24.

Singh, K. R., Nayak, V., Singh, J., Singh, A. K., & Singh, R. P. (2021). Potentialities of bioinspired metal and metal oxide nanoparticles in biomedical sciences. *RSC Advances*, *11*(40), 24722–24746.

Sorbiun, M., Mehr, E. S., Ramazani, A., & Malekzadeh, A. M. (2018). Biosynthesis of metallic nanoparticles using plant extracts and evaluation of their antibacterial properties. *Nanochem Res*, *3*(1), 1–16. https://doi.org/10.22036/ncr.2018.01.001

Srimathi Pasupathy, P., & Manivannan Rajamanickam, R. (2019). Synthesis of pure and

bio modified calcium oxide (CaO) nanoparticles using waste chicken egg shells and evaluation of its antibacterial activity. *International Journal of Pharmaceutical Sciences and Research*, *10*(10), 4731–4737.

Sumathi, V. (2017). *Optical Characterization Of Calcium Oxide Nanoparticles*. 63–67.

Tang, Z. X., Yu, Z., Zhang, Z. L., Zhang, X. Y., Pan, Q. Q., & Shi, L. E. (2013). Sonication-assisted preparation of CaO nanoparticles for antibacterial agents. *Quimica Nova*, *36*(7), 933–936.

Zeid, E. F. A., Ibrahem, I. A., Ali, A. M., & Mohamed, W. A. A. (2019). The effect of CdO content on the crystal structure, surface morphology, optical properties and photocatalytic efficiency of p-NiO/n-CdO nanocomposite. *Results in Physics*, *12*, 562–570.

RESEARCH FUNDS ACKNOWLEDGMENT

This research project is funded by **Adama Science and Technology University (ASTU)** under the **Grant number ASTU/SM-R/770/23**, Adama, Ethiopia.